J. Condensed Matter Nucl. Sci. 36 (2022) 210–246

Recent Progress on Phonon-Nuclear Theoretical Models

Peter L. Hagelstein
Massachusetts Institute of Technology, Cambridge, MA, USA

Abstract

Excess heat in the Fleischmann-Pons experiment presents numerous challenges for theorists, the biggest of which is to account for the absence of energetic nuclear particles in amounts commensurate with the energy produced. Our focus has been on the development of such a model, with recent progress reviewed. To account for excess heat production we contemplate a complicated model based on nuclear excitation transfer, subdivision and the down-conversion of keV nuclear quanta to a large number of phonons. The phonon-nuclear interaction that provides the foundation has been derived from a many-nucleon Dirac formalism, and we discuss recent efforts to confirm and improve upon the derivation. The quantification of the models under consideration require the evaluation of phonon-nuclear matrix elements, with recent progress discussed. The first step in the excess heat model involves the excitation transfer of a 24 MeV quantum associated with the $D_2/^4He$ transition, which motivates a consideration of modeling and connections with experiments showing low-level energetic nuclear emissions. The analogous first step in the case of the 5.5 MeV quantum associated with the $HD/^3He$ transition is considered, where there is the possibility of low-level energetic nuclear emission, and where the issue of the availability of near-resonant energy levels can be studied. A nearby level in ^{137}Cs is identified, which suggests a possible mechanism for the acceleration of the decay rate. We have recently revisited the issue of the null reaction, in which a $D_2/^4He$ transition leads to the production of a compact D_2 state from ^4He, with the conclusion that this may be important in models for excess heat production and for low-level nuclear emission. Progress on subdivision is reviewed, including connections with experiments showing low-level nuclear emission, and candidates for laboratory tests. The possibility of a new $^{57}Co/^{57}Fe$ resonant excitation transfer experiment in a near single crystal sample is presented. A numerical approach for the evaluation of the rate for excess heat production in the models under discussion is discussed.

Keywords: LENR theory, Phonon-nuclear coupling, Excess heat model, Review, Excitation transfer

1. Introduction

For more than three decades following the announcement of excess heat in the Fleischmann-Pons experiment there has been the promise of a small scale clean nuclear energy source [1], [2]. Progress has been hindered due to a lack of resources and manpower, largely due to the belief within the mainstream physics community that the basic effect is inconsistent with nuclear physics and solid-state physics – in essence that there is no possibility that the excess heat effect could be real [3].

One approach to changing things is to develop a (useful) commercial product based on Fleischmann-Pons excess heat, which would once and for all provide an unambiguous demonstration that the effect is real. Quite a few efforts along these lines have over the years met with financial or technical headaches, but the prospects at present seem good that some of these efforts (such as Technova [4]–[6] and Brillouin [7], [8]) will succeed.

We have long focused on the question of how it works [9]–[11] which if solved could help move the experiments and technology development forward. To engage the mainstream scientific community in taking an interest in theoretical and experiment problems in the field has always been a major goal, but in our view this has always been more of a social rather than a scientific issue.

The theoretical challenges associated with how it works have been intimidating from the start. Critics and skeptics initially drew attention to the lack of neutrons and 24 MeV gammas as evidence that dd-fusion did not occur [3], arguing that the source of the energy could not be nuclear. At this point it seems clear that the critics and skeptics did not go far enough – in many experiments considerable energy is detected but there is no evidence for the presence of *any* energetic nuclear particles in amounts consistent with the energy produced (and also no evidence for the much larger amount of chemical reaction products that would be needed to account for the energy). According to the textbooks, energetic nuclear particles must be produced in connection with energy generation as a direct consequence of energy and momentum conservation; hence, their absence would seem to require a violation of energy and momentum conservation at the outset. From our perspective this was the biggest theoretical problem, even though it was not the main focus of the critics early on.

As has been often repeated for more than 30 years the Coulomb barrier between deuterons would be expected to prevent deuteron-deuteron interactions and fusion at the fermi scale in the case of collisions near room temperature, or due to tunneling in molecular D_2 [12]. This argument has been used effectively to rule out excess heat in the Fleischmann-Pons experiment. A focus in connection with this argument was on the rate for incoherent D_2 fusion, which would result in energetic nuclear products such as neutrons – hence, the theoretical argument that this process is too slow to account for the excess heat effect should be understood as being in agreement with experiment. We know that excess heat is not due to tunneling in D_2 leading to incoherent dd-fusion, since the corresponding dd-fusion neutrons are not seen. A better question to have been asked is whether the fusion rate for a mechanism more closely connected with experiment, in particular one which did not result in neutrons or other energetic nuclear particles, could be on the order of what is observed in experiment.

Aside from being the source of theoretical headaches, the absence of commensurate energetic nuclear emissions prevents the reaction mechanism from being studied using conventional nuclear diagnostics. For example, in conventional fusion or fission reactions the energetic nuclear products are detected [13], and from measurements we know a lot about what goes on internally during the reactions. We are not able to make use of the same diagnostics to study the nuclear processes which occur to produce heat in the Fleischmann-Pons experiment, which has prevented an experimental elucidation of the reaction mechanism. For experimental nuclear physicists this gives rise to doubt that excess heat generation has anything to due with nuclear processes.

The theoretical picture which has emerged from our efforts is at once both simple in concept [9]–[11], but complicated in implementation. The theoretical starting place has to be the absence of commensurate energetic nuclear particles, which implies that nature has found a way to take a very large 24 MeV nuclear quantum and split it up into an enormous number of lower energy quanta. Such a thing is unprecedented – while down-conversion as a physical process is certainly known, we have no examples where a large quantum is split up into on the order of 10^9 smaller quanta; yet that seems to be what is needed to account for the experimental results.

This immediately leads to more theoretical headaches. We might expect that a large down-conversion effect might be possible in a strongly coupled quantum system. However, models for nuclei embedded in a solid view the internal nuclear degrees of freedom as largely independent of condensed matter degrees of freedom (such as vibrations or plasmons), with only a weak second-order interaction resulting from perturbations of local electric or magnetic fields. On the face of it the prospects for strong coupling are not encouraging.

All of this emphasizes just how daunting the theoretical issues are, with little help from mechanisms studied in the mainstream literature.

A positive step toward a potential solution came first in the case of new mechanisms for down-conversion. If we consider down-conversion in the case of generalized spin-boson models (or sometimes referred to as Dicke models), an analysis of up-conversion and down-conversion indicates that the indirect coupling between an initial state and final state (where the conversion has been completed) under normal conditions is hindered by destructive interference. Hence, any mechanism capable of reducing or eliminating this destructive interference will result in a dramatic many-orders-of-magnitude increase in the up-conversion and down-conversion rate. In 2002 we noticed that loss asymmetric around the resonant energy point could greatly reduce the destructive interference and dramatically enhance up-conversion and down-conversion [14]–[18]. Models developed to quantify the effect suggested that a down-conversion of a large quantum into on the order of a million smaller quanta was within the realm of possibility. For many years our focus was on this kind of model, until we recognized relatively recently that there needed to be another mechanism (from an initial comparison of theory and experiment from results of excitation transfer experiments) [10], [11]. In this case there is an obscure effect in which the nuclear binding energy varies off of resonance, which can greatly reduce the destructive interference.

Another positive step was the recognition that there could be an alternative coupling mechanism between internal nuclear states and condensed matter modes beyond the weak second-order interaction based on electric and magnetic fields. The idea is that a nucleus embedded in the lattice must be consistent with relativity, undergoing a Lorentz contraction as well as spin and isospin rearrangement when in motion, so that changes in the internal nuclear state when the nucleus moves in connection with lattice vibrations implies a (low-order) relativistic phonon-nuclear interaction [19]. This provides a stronger phonon-nuclear interaction than results from local electric and magnetic fields. It also addresses the conceptual issue of how the small fermi-scale internal nuclear degrees of freedom can interact with lattice vibrations organized on the meso- or macro- scale involving a large number of atoms.

At some point theory needs to connect in a meaningful way with experiment. Ideally, we would like a clean demonstration of the phonon-nuclear interaction in the simplest way possible, which would be in a process where the exchange of a single phonon results in the change of an internal nuclear state. Unfortunately, this doesn't work since relevant phonon energies are much less than 1 eV and relevant nuclear transition energies are greater than 1 keV. Consequently, the lowest-order physical effect that we might study is excitation transfer, in which the excitation in one nucleus is transferred to a different nucleus, with the exchange of (at least) one phonon for each nuclear transition [20]. This second-order process then by necessity becomes the focus of basic experimental studies to clarify the phonon-nuclear interaction. In our lab we have evidence for resonant phonon-mediated nuclear excitation in observations of dynamic angular anisotropy, and observations consistent with nonresonant excitation transfer in delocalization experiments [21]–[23].

The mechanism for accelerated up-conversion or down-conversion mentioned above operates through a large number of sequential non-resonant excitation transfer steps which must occur before the system decoheres. If excitation transfer can be rapid, then there is the possibility of a subdivision effect, in which a few excitation transfer steps starting from an initial excited nuclear state leads to excitation in two or more nuclei at lower energy where the total energy is conserved [10], [11]. An unambiguous demonstration of subdivision in the lab has not yet been accomplished, but it may be that some of the low-level neutron emission seen in experiments with deuterated metals might be a result of subdivision.

As another positive step in the development of a picture for excess heat generation, subdivision provides a bridging mechanism, allowing for some of the down-conversion to take place largely in the nuclei (through subdivision), and the rest of the down-conversion to take place as a multi-phonon process through a coupling of a few nuclear transitions with a highly-excited vibrational mode.

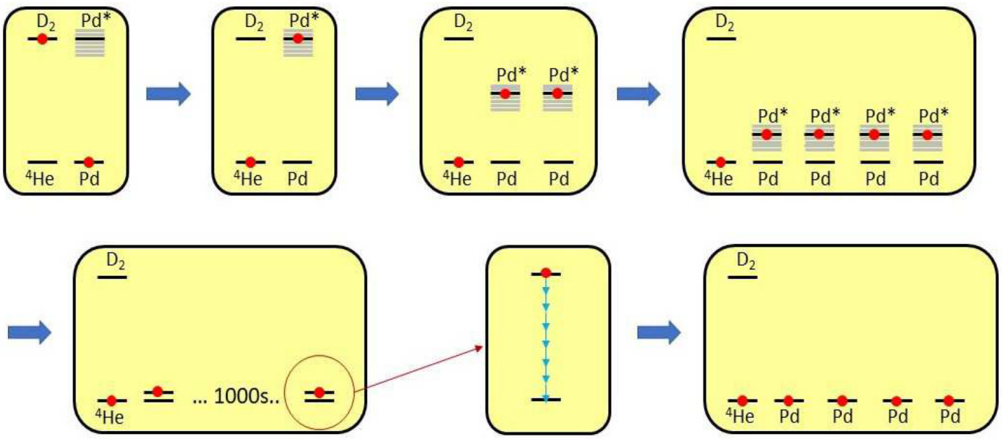

Figure 1. Schematic of the model for excess heat production under consideration. The first step is excitation transfer of 24 MeV from the $D_2/^4$He transition to produce excitation in a Pd nucleus (or other nucleus in the lattice). This is quickly followed by a subdivision step resulting in two excited nuclei with roughly 12 MeV each. More subdivision steps leads ultimately to a thousands of nuclei with much lower levels of excitation – likely involving excited impurity nuclei since the Pd isotopes do not have long-lived low-lying excited states. Finally, this lower nuclear excitation is down-converted into phonons.

The overall picture for excess heat production consistent with these mechanisms is illustrated in Figure 1. It is clear that the overall process is pretty complicated, being made up of many individual theoretical pieces. If the associated dynamics can proceed coherently (in the sense of a coherent quantum process analogous to Rabi oscillations), then there is the possibility of great acceleration in the associated reaction rate. The decay associated with a quantum mechanical incoherent process is governed by the Golden Rule, and the associated rate is quadratic in the coupling matrix element. The dynamics associated with a quantum mechanical coherent process can be linear in the coupling matrix element. For incoherent fusion, the coupling matrix element is hindered by the Gamow factor e^{-G} resulting from tunneling through the Coulomb barrier, so that the reaction rate is proportional to e^{-2G}. If the mechanism outline above proceeds as a coherent quantum process, then the rate can be proportional to e^{-G}. Since e^{-G} is on the order of 10^{-40}, there is the potential for a dramatic acceleration of the reaction rate (and hence fusion rate) due to quantum coherence.

In what follows we review some recent advances in the theory, models, picture, and applications.

2. Lowest-Order Phonon-Nuclear Interaction From the Dirac Model

We consider first the lowest-order phonon-nuclear interaction derived from the Dirac model. As discussed briefly above, the idea is that the internal degrees of freedom of a nucleus are modified as the nucleus moves in connection with lattice vibrations due to relativity, which means that there must be an associated relativistic phonon-nuclear interaction. Our preference would be to make use of a fully covariant model for the derivation of the effect, which the many-body Dirac model with realistic interactions is not. However, the Dirac model is relativistic, it is cast in a Hamiltonian formulation which make a derivation simple, and over many decades of use we know that the Dirac model is capable of capturing a significant part of the relativistic contribution to the quantum problem.

We can start with a many-particle Dirac model in the form

$$\hat{H} \;=\; \sum_j \beta_j mc^2 + \sum_j \boldsymbol{\alpha}_j \cdot c\hat{\mathbf{p}}_j + \sum_{j<k} V_{jk} \tag{1}$$

and then make use of a partial Foldy-Wouthuysen transformation to obtain [19]

$$\begin{aligned} e^{i\hat{S}}\hat{H}e^{-i\hat{S}} \;=\; & \frac{|\hat{\mathbf{P}}|^2}{2M}\sum_j \frac{m_j}{M}\beta_j + \sum_j \beta_j mc^2 + \sum_j \boldsymbol{\alpha}_j \cdot c\hat{\boldsymbol{\pi}}_j + \sum_{j<k} V_{jk} \\ & + \frac{1}{M}\sum_j \beta_j \hat{\mathbf{P}}\cdot\hat{\boldsymbol{\pi}}_j + \frac{1}{2Mc}\sum_j \Big[(\beta_j\boldsymbol{\alpha}_j + \beta_k\boldsymbol{\alpha}_k)\cdot\hat{\mathbf{P}}, V_{jk}\Big] \\ & + \cdots \end{aligned} \tag{2}$$

What this transformation does is to provide for an approximate separation of the center of mass degrees of freedom (as a nonrelativistic problem) and relative degrees of freedom (as a relativistic problem). On the first line are terms that can be interpreted as the center of mass kinetic energy, a relative Hamiltonian for the internal nuclear states, and low-order terms that provide a coupling between the center of mass and relative degrees of freedom.

The lowest-order phonon-nuclear interaction describing single phonon exchange from this model is

$$\hat{H}_{int} \;=\; \hat{\mathbf{a}} \cdot c\hat{\mathbf{P}} \tag{3}$$

where the center of mass momentum $\hat{\mathbf{P}}$ for a nucleus in a condensed matter environment is an operator made of up phonon creation and annihilation operators, and where $\hat{\mathbf{a}}$ is an operator which acts on the internal nuclear degrees of freedom for consistency with the Dirac model version of relativity. The $\hat{\mathbf{a}}$ operator is given by

$$\hat{a} \;=\; \frac{1}{Mc}\sum_j \beta_j \hat{\boldsymbol{\pi}}_j + \frac{1}{2Mc^2}\sum_j \Big[(\beta_j\boldsymbol{\alpha}_j + \beta_k\boldsymbol{\alpha}_k), V_{jk}\Big]. \tag{4}$$

3. Unsuccessful Effort to Correct the Many-Particle Dirac Model

The relativistic phonon-nuclear interaction mentioned above provides one foundation for the models under discussion. Consequently, a concern is that this interaction does not appear to be known in the mainstream literature, and we have been concerned that it may not be a real physical effect. A headache is that our derivation of the effect is from a model based on a many-particle Dirac model, and it is well known that the many-particle Dirac model with realistic interaction is not covariant.

One way to proceed might be through the development of a modified many-particle Dirac model which is corrected in order to make it more covariant. The thought was that this might clarify whether the proposed phonon-nuclear interaction is real, or an artifact of the many-particle Dirac model. A substantial effort was put into the problem, ultimately without success. It seems useful to give an account of the ideas and issues here.

To make a version of the many-particle Dirac model that is more nearly covariant, what is needed is a consistent set of operators for the many-particle system $\hat{H}$, $\hat{\mathbf{P}}$, $\hat{\mathbf{J}}$ and $\hat{\mathbf{K}}$ associated with translations in time, space, rotational angle and momentum. Poincaré invariance requires that these operators satisfy [24]–[28]

$$[\hat{P}_i, \hat{P}_j] \;=\; 0 \quad [\hat{P}_i, \hat{H}] \;=\; 0 \quad [\hat{J}_i, \hat{H}] \;=\; 0$$

$$[\hat{J}_i, \hat{J}_j] \;=\; i\hbar\epsilon_{ijk}\hat{J}_k \quad [\hat{J}_i, \hat{P}_j] \;=\; i\hbar\epsilon_{ijk}\hat{P}_k \quad [\hat{J}_i, \hat{K}_j] \;=\; i\hbar\epsilon_{ijk}\hat{K}_k$$

$$[\hat{K}_i, \hat{P}_j] \;=\; i\hbar\delta_{ij}\frac{1}{c^2}\hat{H} \quad [\hat{K}_i, \hat{K}_j] \;=\; -i\hbar\epsilon_{ijk}\frac{1}{c^2}\hat{J}_k \quad [\hat{K}_i, \hat{H}] \;=\; i\hbar\hat{P}_i \tag{5}$$

Strictly speaking, such coupled commutation relations are quite difficult to solve in general. For the special case of a many-particle Pauli model, a solution by construction was found for a Pauli type of formulation (in which spins are included, but not involving 4-vectors) by Foldy [29], and by Krajcik and Foldy [30].

Krajcik and Foldy noted that the most important of the commutation relations was the one involving boost and Hamiltonian, which we can write as

$$[\hat{\mathbf{K}}, \hat{H}] \;=\; i\hbar\mathbf{P} \tag{6}$$

In one attack on the problem we sought to develop a solution based on matching orders according to

$$\hat{H} \;=\; \hat{H}_{+2} + \hat{H}_0 + \hat{H}_{-2} + \cdots$$

$$\mathbf{K} \;=\; \mathbf{K}_0 + \mathbf{K}_{-2} + \mathbf{K}_{-4} + \cdots \tag{7}$$

Guided in part by the work of Krajcik and Foldy, after some experimentation we worked with Hamiltonian and boost operators for the two-body version of the problem, trying a variety of different operators. A specific example makes use of a Hamiltonian operator according to

$$\hat{H}_2 \;=\; m_1c^2\beta_1 + m_2c^2\beta_2$$

$$\hat{H}_0 \;=\; \boldsymbol{\alpha}_1\cdot c\mathbf{p}_1 + \boldsymbol{\alpha}_2\cdot c\mathbf{p}_2 + V_{12}$$

$$\hat{H}_{-2} \;=\; -\left[\frac{\beta_1\boldsymbol{\alpha}_1\cdot c\mathbf{p}_1}{2m_1c^2} + \frac{\beta_2\boldsymbol{\alpha}_2\cdot c\mathbf{p}_2}{2m_2c^2}, V_{12}\right]$$

$$\hat{H}_{-4} \;=\; \frac{1}{2}\left[\frac{\beta_1\boldsymbol{\alpha}_1\cdot c\mathbf{p}_1}{2m_1c^2} + \frac{\beta_2\boldsymbol{\alpha}_2\cdot c\mathbf{p}_2}{2m_2c^2}, \left[\frac{\beta_1\boldsymbol{\alpha}_1\cdot c\mathbf{p}_1}{2m_1c^2} + \frac{\beta_2\boldsymbol{\alpha}_2\cdot c\mathbf{p}_2}{2m_2c^2}, V_{12}\right]\right]$$
$$-\frac{1}{8c^2}\left(\frac{|\mathbf{p}_1|^2V_{12} + V_{12}|\mathbf{p}_1|^2}{m_1^2} + \frac{|\mathbf{p}_2|^2V_{12} + V_{12}|\mathbf{p}_2|^2}{m_2^2}\right) \tag{8}$$

and a boost operator given by:

$$\mathbf{K}_0 \;=\; \mathbf{r}_1\beta_1m_1 + \mathbf{r}_2\beta_2m_2 \tag{9}$$

$$\mathbf{K}_{-2} \ = \ \frac{1}{2c^2}\Big(\mathbf{r}_1(\boldsymbol{\alpha}_1\cdot c\mathbf{p}_1)+(\boldsymbol{\alpha}_1\cdot c\mathbf{p}_1)\mathbf{r}_1+\mathbf{r}_2(\boldsymbol{\alpha}_2\cdot c\mathbf{p}_2)+(\boldsymbol{\alpha}_2\cdot c\mathbf{p}_2)\mathbf{r}_2\Big)+\frac{1}{4c^2}\Big(\mathbf{r}_1V_{12}+V_{12}\mathbf{r}_1+\mathbf{r}_2V_{12}+V_{12}\mathbf{r}_2\Big)$$

$$\mathbf{K}_{-4} \ = \ -\frac{1}{2c^2}\left[\frac{\beta_1\boldsymbol{\alpha}_1\cdot c\mathbf{p}_1}{2m_1c^2}+\frac{\beta_2\boldsymbol{\alpha}_2\cdot c\mathbf{p}_2}{2m_2c^2},V_{12}(\mathbf{r}_1+\mathbf{r}_2)\right]$$

$$\mathbf{K}_{-6} \ = \ \frac{1}{4}\left[\frac{\beta_1\boldsymbol{\alpha}_1\cdot\mathbf{p}_1}{2m_1c^2}+\frac{\beta_2\boldsymbol{\alpha}_2\cdot\mathbf{p}_2}{2m_2c^2},\left[\frac{\beta_1\boldsymbol{\alpha}_1\cdot\mathbf{p}_1}{2m_1c^2}+\frac{\beta_2\boldsymbol{\alpha}_2\cdot\mathbf{p}_2}{2m_2c^2},V_{12}(\mathbf{r}_1+\mathbf{r}_2)\right]\right] \tag{10}$$

For the commutation relation at different orders we found

$$[\mathbf{K},\hat{H}]_{+2} \ = \ [\mathbf{K}_0,\hat{H}_{+2}] \ = \ \left[\mathbf{r}_1\beta_1m_1+\mathbf{r}_2\beta_2m_2, m_1c^2\beta_1+m_2c^2\beta_2\right] \ = \ 0 \tag{11}$$

$$[\mathbf{K},\hat{H}]_0 \ = \ [\mathbf{K}_0,\hat{H}_0]+[\mathbf{K}_{-2},\hat{H}_{+2}] \ = \ 0 \tag{12}$$

$$[\mathbf{K},\hat{H}]_{-2} \ = \ [\mathbf{K}_0,\hat{H}_{-2}]+[\mathbf{K}_{-2},\hat{H}_0]+[\mathbf{K}_{-4},\hat{H}_{+2}] \ = \ i\hbar\mathbf{P} \tag{13}$$

$$\begin{aligned}[\mathbf{K},\hat{H}]_{-4} \ &= \ [\mathbf{K}_0,\hat{H}_{-4}]+[\mathbf{K}_{-2},\hat{H}_{-2}]+[\mathbf{K}_{-4},\hat{H}_0]+[\mathbf{K}_{-6},\hat{H}_2] \ = \\ &+\frac{1}{4m_1c^2}\beta_1\left[\boldsymbol{\alpha}_1\cdot\hat{\mathbf{p}}_1\mathbf{r}_1\boldsymbol{\alpha}_1\cdot\hat{\mathbf{p}}_1,\hat{V}\right]+\frac{1}{4m_2c^2}\beta_2\left[\boldsymbol{\alpha}_2\cdot\hat{\mathbf{p}}_2\mathbf{r}_2\boldsymbol{\alpha}_2\cdot\hat{\mathbf{p}}_2,\hat{V}\right] \\ &-\frac{1}{4m_1c^2}\beta_1\mathbf{r}_2\left[|\mathbf{p}_1|^2,\hat{V}\right]-\frac{1}{4m_2c^2}\beta_2\mathbf{r}_1\left[|\mathbf{p}_2|^2,\hat{V}\right]\end{aligned} \tag{14}$$

For this model we assumed that the potential satisfies

$$[\beta_1,\hat{V}] \ = \ [\beta_2,\hat{V}] \ = \ 0 \tag{15}$$

as well as

$$[\mathbf{r}_1,\hat{V}] \ = \ [\mathbf{r}_2,\hat{V}] \ = \ 0 \tag{16}$$

We were not able to develop a consistent matching of terms at all orders using this approach. Interestingly enough, it is possible to obtain models which are more covariant than the two-body Dirac model as measured by deviations from the commutators from zero at higher order (as this one is). The corrections to the potential are similar in this kind of construction to those found by Krajcik and Foldy.

A two-body Dirac model with improved covariance would seem to be an important result, and worth further consideration. We were very interested as a first application of the corrected model to see what happened to the phonon-nuclear coupling terms. Consistent with our worst fears, the lowest-order phonon-nuclear interaction involving the potential is cancelled out by the new correction terms. This appeared to suggest that the phonon-nuclear coupling interaction obtained from the many-particle Dirac model is an artifact, and that the interaction goes away when corrected to be more covariant.

However, there is a problem in this argument that needs to be thought about. If we view the problem as a mathematical problem, then we have succeeded in developing versions of the two-body Dirac model which are objectively more covariant, and in a physical system governed by the resulting Hamiltonian the lowest order potential contribution to the phonon-nuclear interaction vanishes. However, if we view the problem as a physics problem, then through this construction we have added corrections to the potential, and the question might be asked whether the new terms correspond to things that are measured in the lab. In this case the corrections needed to improve covariance correspond to low-order interactions that are not observed experimentally.

The conclusion at this point is that two-body Dirac models with improved covariance that we found developed using this approach involve interactions that are not physical.

There are additional subtleties with this approach. One is that even if operators are constructed that satisfy the commutation relations, it is possible for the solutions to be non-covariant. An example of this is for non-interacting particles with different masses, where in the $+-$ and $-+$ sectors the energy-momentum relation is not covariant. This might provide additional support for not including not including mixed sector solutions in general in connection with physical systems for the many-particle Dirac model. It is possible that the Poincare commutation relations over-constrain the model, since at the end of the day covariance is only needed in the positive energy sector.

4. Thinking About the Foldy and Krajcik-Foldy Transformations

Even though the approach outlined above did not pan out, the development of two-body and many-body Dirac models corrected to be more nearly covariant remains of interest. This led to a consideration of making use of a transformation similar to what was pioneered by Foldy [29] and by Krajcik and Foldy [30] (but applying it to the two-body Dirac model).

The basic idea is to start with a Hamiltonian $\hat{H}$ expressed in terms of individual particle positions and momenta, and then rotate to produce a rotated Hamiltonian $\hat{H}'$ expressed in terms of center of mass and relative positions and momenta:

$$e^{i\hat{S}}\hat{H}(\mathbf{r}_1, \mathbf{r}_2, \hat{\mathbf{p}}_1, \hat{\mathbf{p}}_2)e^{-i\hat{S}} \ = \ \hat{H}'(\mathbf{r}, \mathbf{R}, \hat{\mathbf{p}}, \hat{\mathbf{P}}) \tag{17}$$

where $\mathbf{r}_j$ and $\hat{\mathbf{p}}_j$ are individual particle position and momentum operators, where $\mathbf{r}$ and $\hat{\mathbf{p}}$ are relative operators and where $\mathbf{R}$ and $\hat{\mathbf{P}}$ are center of mass operators. Ideally the Hamiltonian $\hat{H}$ would be the two-body Dirac model with a correction

$$\hat{H} \ = \ \beta_1 mc^2 + \beta_2 mc^2 + \alpha_1 \cdot c\hat{\mathbf{p}}_1 + \alpha_2 \cdot c\hat{\mathbf{p}}_2 + V_{12} + \delta\hat{H} \tag{18}$$

where $\delta\hat{H}$ would make the resulting model more nearly covariant. The rotated Hamiltonian $\hat{H}'$ would ideally involve a covariant combination of the at rest Hamiltonian (perhaps with a rotation) and center of mass energy.

In the event that the potential is set to zero, it is possible to develop this kind of transformation exactly, since the two-body Dirac equation is covariant (if the masses are equal). We have developed a construction of this kind at different orders based on

$$e^{i\hat{S}}\left(\beta_1 mc^2 + \beta_2 mc^2 + \alpha_1 \cdot c\hat{\mathbf{p}}_1 + \alpha_2 \cdot c\hat{\mathbf{p}}_2\right)e^{-i\hat{S}} \ = \ \hat{H}' \tag{19}$$

where the part of the rotated Hamiltonian in the positive energy sector is consistent with [31]

$$\left(\hat{H}'\right)_{++} = \sqrt{(Mc^2)^2 + 4c^2|\hat{\mathbf{q}}|^2 + c^2|\hat{\mathbf{P}}|^2} \tag{20}$$

with

$$\hat{\mathbf{q}} = \hat{\mathbf{p}} - \frac{1}{2}\frac{\hat{\mathbf{p}}\cdot\hat{\mathbf{P}}}{(Mc)^2 + |\hat{\mathbf{p}}|^2}\hat{\mathbf{P}} + \cdots \tag{21}$$

An interpretation is possible that $\hat{\mathbf{q}}$ is the Dirac model's version of the relative momentum in the moving frame. After experimenting with a large number of approaches that uniformly failed, it was encouraging to see that this construction could be carried out reasonably for this simple model.

The generalization of the approach to include a potential on the face of it appears to be straightforward – we have carried out such a construction for several orders. The initial conclusion based on this exploratory calculation is that a rotation is possible resulting in a transformed Hamiltonian consistent with covariance up to higher order than we were expecting (and higher order than is obtained from numerical calculations). The headache is that at each point in the construction terms appear which could be treated as covariant corrections to the Hamiltonian, or which can be rotated out (so that their impact is deferred to higher order) – and we are not yet able to identify what the lowest-order correction should be.

The conclusion for now is that it should be possible to develop a version of the two-body Dirac model where the lowest-order covariant correction can be identified. An issue is that it is possible that corrections which improve covariance may also be nonphysical. Another issue is that requiring overall covariance in this case may over-constrain the system as once again covariance is only required for the positive energy sector.

5. Exploratory Numerical Solutions

In connection with the models investigated above, we developed a finite basis code to solve the two-body Dirac model with a scalar SHO potential in order to gain some insight as to how much the lack of covariance of the model impacted the eigenvalues for a composite in motion. The results were interesting.

We found that the energy-momentum relation for the ground state in the positive energy sector was very nearly consistent with covariance (the numerical and analytic covariant solutions cannot be distinguished for the parameters studied as shown in Figure 2), which is encouraging [31]. We also found that (minor) nonphysical changes in the level splitting occurred in the moving frame. Of concern is that the deviations from covariance occur at the same order ($|\mathbf{P}|^2$) as would occur with the term giving rise to the phonon-nuclear interaction.

What remains to be done is to examine potential candidates for correction terms, and then to verify numerically whether they are effective or not. At this point we are beginning to suspect that the lack of covariance is a consequence of using a Hamiltonian formulation, and that corrections that improve covariance are nonphysical.

6. Phonon-Nuclear Interaction From a Covariant Model

From the discussion above it might be concluded that the many-particle Dirac model is good enough to allow a derivation of the phonon-nuclear interaction at low order, but the lack of covariance probably precludes a treatment at high order and doubt remains as to whether the low-order interaction derived is physical. This motivates interest in whether the interaction can be derived from a covariant model.

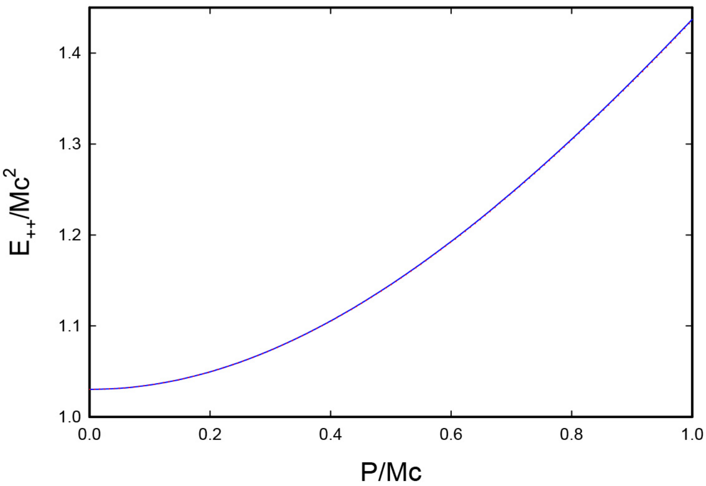

Figure 2. Numerical (blue) and analytic covariant (red) ground state energy as a function of the center of mass momentum for a two-body Dirac model with an SHO potential with $\hbar\omega_0/Mc^2 = 0.02$.

One such model is the covariant two-body Bethe-Salpeter model, which for us is an obvious candidate with which to examine the issue. We worked with a version of this model in a form close to the two-body Dirac model described above, and make use of a partial Foldy-Wouthuysen transformation which leads to an approximate separation of the (nonrelativistic) center of mass degrees of freedom and (relativistic) relative degrees of freedom. The model that results includes terms which are close to those derived from the two-body Dirac model. In this case the kernel describing the interaction is transformed according to [31]

$$V'(\mathbf{k},\epsilon) \; = \; V(\mathbf{k},\epsilon) + \frac{1}{2Mc}\left[\beta_1\boldsymbol{\alpha}_1 + \beta_2\boldsymbol{\alpha}_2, V(\mathbf{k},\epsilon)\right] \cdot \hat{\mathbf{P}} + \cdots \tag{22}$$

This compares well with the lowest-order interaction due to the potential obtained from the two-body Dirac model

$$\hat{H}_{int} \; = \; \frac{1}{2Mc}\left[\beta_1\boldsymbol{\alpha}_1 + \beta_2\boldsymbol{\alpha}_2, V(|\mathbf{r}_2 - \mathbf{r}_1|)\right] \cdot \hat{\mathbf{P}} \tag{23}$$

It is very encouraging that the phonon-nuclear interaction can be derived from a covariant model, and that the lowest-order interaction is essentially the same as obtained from the two-body Dirac model.

7. Progress on Matrix Element Calculations

A quantification of the models under discussion in this paper requires the evaluation of phonon-nuclear matrix elements, as well as the estimation of off-resonant energy shifts. Years ago we made use of Pauli reduction to develop an estimate for the phonon-nuclear matrix element for the $D_2/^4He$ transition [32]. A better approach to this problem would be to develop a reduction for the phonon-nuclear interaction, and to develop a more standard calculation. An early attempt as this kind of model was carried out for the spin-orbit contribution to the phonon-nuclear matrix element in the case of the 6.2 keV transition of ^{181}Ta [33].

7.1. Nonrelativistic Reduction

The phonon-nuclear interaction discussed above is given in terms of relativistic operators; however, most nuclear structure calculations these days are done in the context of a nonrelativistic description with nonrelativistic interactions that are derived from a covariant field theory (chiral effective field theory) model [34]–[37]. It would be possible to make use of the relativistic phonon-nuclear interaction in connection with the relativistic interactions from this model, and then reduce the expressions that result to a form appropriate for a nonrelativistic calculation.

This has recently been done for the relativistic one-pion exchange potential based on the spatial part of the pseudovector interaction, which is consistent with the lowest-order interaction from chiral effective field theory [38]. For the one-phonon exchange contribution this can be written as

$$\left(\hat{H}'_{int}(j,k)\right)_{NR} = -\frac{1}{4Mmc^2}\left[\boldsymbol{\sigma}_j \cdot \mathbf{p}_j, \left[\boldsymbol{\sigma}_j \cdot \mathbf{P}, \hat{V}_{jk}^{(NR)}\right]\right] - \frac{1}{4Mmc^2}\left[\boldsymbol{\sigma}_k \cdot \mathbf{p}_k, \left[\boldsymbol{\sigma}_k \cdot \mathbf{P}, \hat{V}_{jk}^{(NR)}\right]\right] \tag{24}$$

where $\hat{V}_{jk}^{(NR)}$ is the nonrelativistic one-pion exchange interaction.

7.2. Progress on the HD/^{3}He Phonon-Nuclear Matrix Element

One of the more straightforward calculations to be done is the evaluation of the phonon-nuclear matrix element in the case of the HD/^{3}He transition, which is important for models under discussion for excess heat in the NiH system. A construction for the molecular HD states and doublet S component for the ^{3}He state is given in [39], along with a reduction of the spin, isospin, and angular degrees of freedom. The resulting matrix elements are in terms of relative radial coordinates, which are convenient for numerical evaluation. The plan is to develop estimates based on simple approximate radial wave functions, and afterward to attempt a more sophisticated calculation based on an optimized three-body solution for the ^{3}He nucleus.

There are many issues associated with such models. In an ideal situation one would like to work with a phonon-nuclear operator that is consistent with the potential used. This would suggest that we should start with molecular HD and ^{3}He states evaluated with the chiral effective field theory model, and then develop reductions for the LO, NLO and NNLO potentials [37] needed for the structure calculations. This would constitute a major theoretical project. It would take much less work to make use of the same structure calculation, but then use only the lowest-order (LO) interaction for the phonon-nuclear matrix element, with an associated loss of accuracy. Less work would be required to develop wave functions based on older empirical potentials for the matrix elements, but then there is the issue of developing a consistent phonon-nuclear interaction (since the older empirical potentials were not relativistic). In this case one could make do with the LO contribution to the phonon-nuclear interaction in the large r regime, which would pick up some of the contributions to the matrix element.

7.3. Progress on Models for Transitions in Heavier Nuclei

We would like to use or develop codes that can provide wave functions for heavier nuclei that could be used for the systematic evaluation of phonon-nuclear matrix elements. Developing single configuration wave functions is straightforward based on effective interactions (such as the Skyrme interaction [40]). However, correlation is important in structure calculations, and single configuration models in general do not give good results for E1, M1 or E2 matrix elements for low-energy transitions. Much progress has been made including correlation through the development of multiconfigurational structure models based on effective interactions (see [41] as an example of a substantial literature on this problem). Codes (such as ANTOINE [41]) are available for this type of calculation, and there is the possibility of developing a post-processor for phonon-nuclear matrix element calculations.

We have considered the development of this kind of code for some exploratory calculations. In the case of the LO chiral effective field theory interaction we can write the potential in coordinate space as

$$v_{LO}(\mathbf{r}) \ = \ \frac{\mu_\pi c^2}{\kappa^3}\bigg(C'_S + C'_T(\boldsymbol{\sigma}_1\cdot\boldsymbol{\sigma}_2) + \frac{1}{3}f^2_{\pi NN}(\boldsymbol{\tau}_1\cdot\boldsymbol{\tau}_2)(\boldsymbol{\sigma}_1\cdot\boldsymbol{\sigma}_2)\bigg)v_{contact}(r)$$

$$-f^2_{\pi NN}\frac{\mu_\pi c^2}{\kappa^3}(\boldsymbol{\tau}_1\cdot\boldsymbol{\tau}_2)\frac{\boldsymbol{\sigma}_1\cdot\boldsymbol{\sigma}_2}{3}v_{central}(r)$$

$$-f^2_{\pi NN}\frac{\mu_\pi c^2}{\kappa^3}(\boldsymbol{\tau}_1\cdot\boldsymbol{\tau}_2)\bigg(\frac{(\boldsymbol{\sigma}_1\cdot\mathbf{r})(\boldsymbol{\sigma}_2\cdot\mathbf{r})}{r^2} - \frac{\boldsymbol{\sigma}_1\cdot\boldsymbol{\sigma}_2}{3}\bigg)v_{tensor}(r) \tag{25}$$

For multiconfigurational calculations we require a reduction of the interaction in the case of simple (m-scheme [41]) basis states. For example, in the case of the central potential we can write for the central contribution to the general matrix element

$$\bigg\langle a,b\bigg| - f^2_{\pi NN}\frac{\mu_\pi c^2}{\kappa^3}(\boldsymbol{\tau}_1\cdot\boldsymbol{\tau}_2)\frac{\boldsymbol{\sigma}_1\cdot\boldsymbol{\sigma}_2}{3}v_{central}(r)\bigg|a,b\bigg\rangle \ =$$

$$-\frac{1}{3}f^2_{\pi NN}\frac{\mu_\pi c^2}{\kappa^3}\bigg\langle|\tau,m_{\tau a}\rangle_1|\tau,m_{\tau b}\rangle_2\bigg|(\boldsymbol{\tau}_1\cdot\boldsymbol{\tau}_2)\bigg||\tau,m_{\tau c}\rangle_1|\tau,m_{\tau d}\rangle_2\bigg\rangle$$

$$\sum_l\int_0^\infty\int_0^\infty P_a(r_1)P_b(r_2)v_l^{central}(r_1,r_2)P_c(r_1)P_d(r_2)dr_1dr_2$$

$$\sum_{m_a}\sum_{m_b}\sum_{m_c}\sum_{m_d}\sum_m 4\pi(-1)^m\langle l_a,m_a|Y_{l,-m}|l_c,m_c\rangle\langle l_b,m_b|Y_{l,m}|l_d,m_d\rangle$$

$$\sum_{m_{sa}}\sum_{m_{sb}}\sum_{m_{sc}}\sum_{m_{sd}}\bigg\langle|s,m_{sa}\rangle_1|s,m_{sb}\rangle_2\bigg|(\boldsymbol{\sigma}_1\cdot\boldsymbol{\sigma}_2)\bigg||s,m_{sc}\rangle_1|s,m_{sd}\rangle_2\bigg\rangle$$

$$\langle j_a,m_{ja}|l_a,m;s,m_{sa}\rangle\langle j_b,m_{jb}|l_b,m;s,m_{sb}\rangle\langle l_c,m;s,m_{sc}|j_c,m_{jc}\rangle\langle l_d,m;s,m_{sd}|j_d,m_{jd}\rangle \tag{26}$$

At this point reductions have been developed for the Skyrme interaction, for the one-pion exchange potentials, and for the LO and NLO potentials from chiral effective field theory.

With luck we will have some numerical results for phonon-nuclear matrix elements for problems of interest in the coming year.

8. Excitation Transfer of a 24 MeV Quantum

As discussed in the introduction, the overall process for excess heat production in the picture under consideration is quite complicated. Since energetic particles are not seen in amounts commensurate with the energy produced, we are not able to study the excess heat process when it is producing excess heat using standard nuclear particle detection.

Consider the first step of the proposed reaction process outlined in the introduction, which involves the transfer of 24 MeV to a (reasonably stable) highly excited state of a nucleus in the host lattice (either a Pd nucleus, or an impurity nucleus). When excess heat is produced, the thought is that excitation in this highly excited state is rapidly transferred elsewhere through excitation transfer processes associated with subdivision. If these excitation transfer processes are fast compared to the lifetime of the highly excited nuclear state, then very little in the way of disintegration products would be seen. It may be that the excitation is rapidly transferred to a longer-lived highly excited state prior to subdivision, perhaps one with more angular momentum, which would also hinder the detection of decay products.

8.1. Excitation Transfer to Pd

Suppose now that there is a problem so that the reaction proceeds much more slowly. For example, suppose that the highly-excited phonon mode is insufficiently excited, or that the number of D_2 dideuterium species is low, or perhaps that there are insufficient impurity nuclei present in the lattice with reasonably stable low-lying excited states. In this case it may be that the highly excited nucleus decays a larger fraction of the time [20], as illustrated for ^{106}Pd in Figure 3.

We conjectured previously [20] that the energetic alphas produced this way may be the source of the signals seen in Ref. [42], and that the 14 MeV neutrons from this process may be the source of energetic neutrons commented on in Ref. [43].

8.2. Systematics

Whether this mechanism is responsible for some of the energetic nuclear particles observed in experiments is at present not confirmed; however, a confirmation (or disproof) is possible since the alpha energies have a strong dependence on nuclear mass [20] (as shown in Figure 4).

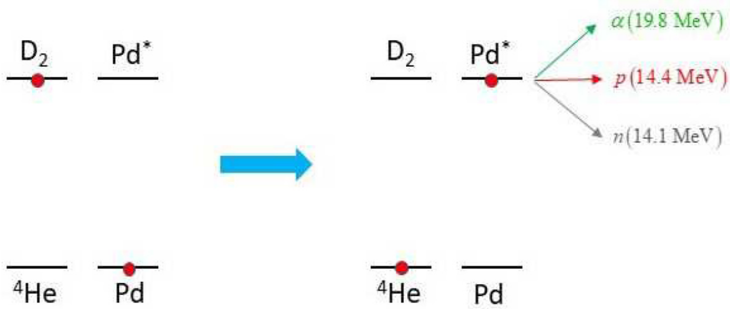

Figure 3. Schematic of excitation transfer of 24 MeV from the D_2/^{4}He transition resulting in a highly-excited state in ^{106}Pd that subsequently decays.

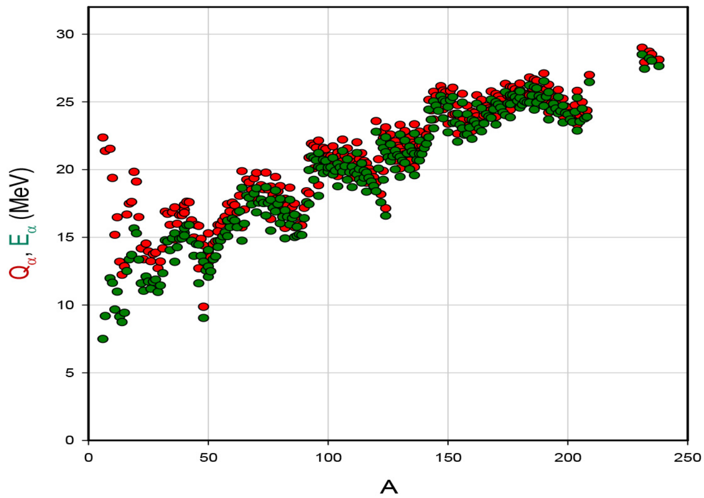

Figure 4. Reaction energy Q (red) and alpha energy E_α (green) for $D_2/^4He$ excitation transfer to isotopes with different nuclear mass A.

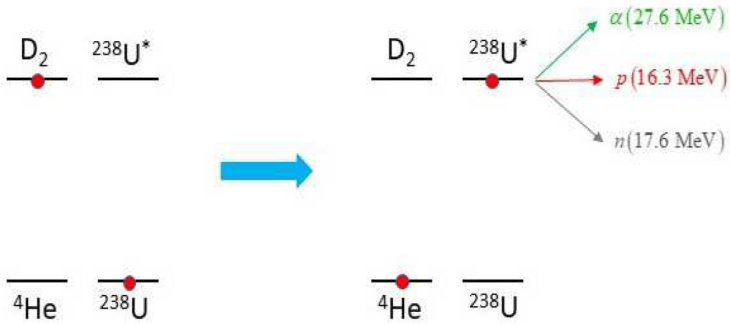

Figure 5. Schematic of excitation transfer of 24 MeV from the $D_2/^4He$ transition resulting in a highly-excited state in ^{238}U that subsequently decays.

This suggests that looking for energetic alpha emission from elements with high Z might be an important goal, as the confirmation of an energetic 27.6 MeV alpha from ^{238}U (see Figure 5) would strongly support the proposed mechanism.

8.3. Excitation Transfer to Ti

Chambers and co-workers reported the observation of charged particles near 5 MeV in the case of deuteron ion bombardment of Ti at low energy (350 eV) [44], [45]. In Table 1 is listed the various candidate reaction particles possible associated with decay of highly excited states in the Ti isotopes following the excitation transfer of a 24 MeV quantum from the $D_2/^4He$ transition.

Table 1. Energies (MeV) for neutrons, protons, deuterons, tritons, ^{3}He, and ^{4}He (including recoil) expected from the decay of the different stable Ti isotopes following excitation transfer of a 24 MeV quantum from the $D_2/^4He$ transition.

isotope	E_n	E_p	E_d	E_t	E_{3He}	E_{4He}
^{46}Ti	10.42	13.21	4.21	0.89	2.99	14.46
^{47}Ti	14.64	13.09	6.55	1.66	5.10	13.62
^{48}Ti	11.96	12.14	3.81	1.38	1.16	13.20
^{49}Ti	15.38	12.24	6.22	1.97	3.28	12.55
^{50}Ti	12.65	11.45	3.63	1.69	–	12.08

Note that ^{47}Ti has the possibility of emitting a ^{3}He at 5.10 MeV resulting from this kind of excitation transfer. Not much is known about the specific highly-excited nuclear states in the titanium isotopes in the vicinity of 24 MeV; however, we would expect that reasonably long-lived states that are nearly resonant with the transition energy would be favored. This suggests a scenario in which ^{47}Ti might be special in this sense, which might the emission in this channel to dominate.

This possibility could be pursued by making use of an isotopically pure sample made of ^{47}Ti, and perhaps a sample with ^{47}Ti excluded, which may be able to help sort whether the reaction mechanism proposed here is consistent with experiment. Also, it would be helpful to attempt charged particle detection at higher energy to look for alpha and proton emission. In the data there seems to be no sign of a deuteron signal at 6.55 MeV (the upper energy for which data is given is about 6.2 MeV), which should be clarified by extending range over which ions are detected.

9. Excitation Transfer of a 5.5 MeV Quantum

The picture outlined above for excess heat in PdD can be extended to excess heat in NiH systems under the assumption that the process starts with an HD/^{3}He transition instead of a $D_2/^4He$ transition. If so, then ^{3}He should be observed in amounts commensurate with the energy produced. At this point we are not certain that ^{3}He is the product of light water excess heat, as there are at present no reports where appropriate high-resolution quadrupole mass spectrometry has been used to assay for ^{3}He. From a theoretical perspective we consider this proposed modification of the picture to be a strong candidate for excess heat in light water systems.

9.1. Systematics

The possibility of the excitation transfer of a 5.5 MeV quantum, which is implied as a first step in an excess heat model, can be tested experimentally by looking for decay products from highly-excited nuclear states that are produced following excitation transfer from the HD/^{3}He transitions in a system where excess heat production is frustrated [20]. Once again the expected alpha energies depend strongly on the nuclear mass A as illustrated in Figure 6 – although in this case the more energetic alphas potentially produced at high Z are hindered by the Coulomb barrier. Consequently, alpha emission is expected only in the case of excitation transfer to low A target nuclei; for high A nuclei gamma emission should be sought, unless neutron decay is energetically allowed.

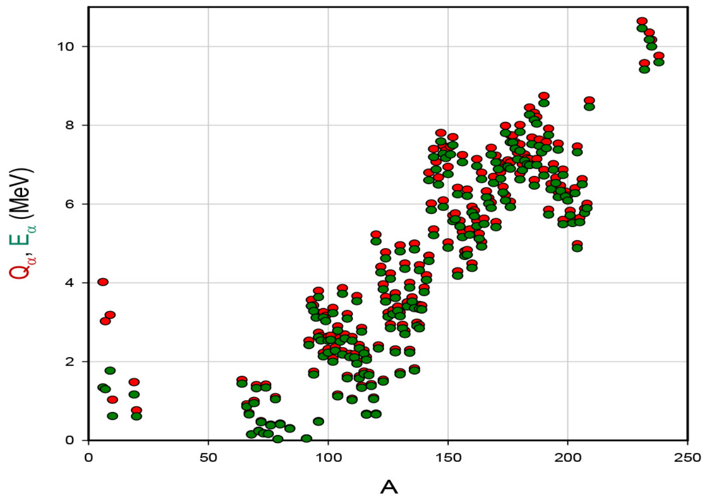

Figure 6. Reaction energy Q (red) and alpha energy E_α (green) for HD/^{3}He excitation transfer to isotopes with different nuclear mass A.

9.2. Proton Emission From ^{6}Li

Of special interest in connection with this discussion is excitation transfer to ^{6}Li according to [20]

$$\left[\text{H+D} \rightarrow {}^3\text{He} + 5.49 \text{ MeV} \right] + \left[{}^6\text{Li} \rightarrow \text{p} + {}^5\text{He} - 4.43 \text{ MeV} \right] + 1.06 \text{ MeV}$$

which is the only example of a proton decay channel starting with a stable ground state nucleus available for the transfer of a 5.5 MeV quantum. We have proposed that this reaction is responsible for the proton signal reported in [46], [47].

10. Resonance Issues for the HD/^{3}He Transition

For excitation transfer from the HD/^{3}He transition near 5.5 MeV the issue of resonance becomes more important, as there are far fewer nuclear states available than for the D_2/^{4}He transition near 24 MeV. At this lower energy there are available detailed lists of nuclear states which have been observed, and which might be candidates for excitation transfer.

10.1. Excited Nuclear States in the Stable Ni Isotopes

Consider excess heat production in and Ni experiment where the first step in the associated reaction picture might be the transfer of a 5.5 MeV quantum to a highly-excited state in a nickel isotope. In this case we can make use of the excited states of the nickel isotopes tabulated in the NUDAT2 database [48], [49] (that extends above 5.5 MeV) to create Figure 7. There are many states in the general vicinity of the HD/^{3}He transition energy, as can be seen in this figure, with the highest density of states associated with ^{61}Ni.

A detailed comparison leads to the conclusion that the nearest state is off of resonance by more than 5 keV (the closest is ^{62}Ni(5488) which compares with the HD/^{3}He transition at 5493.4780 keV), a mismatch which is much too large to be made up through the exchange of a few phonon or plasmon quanta.

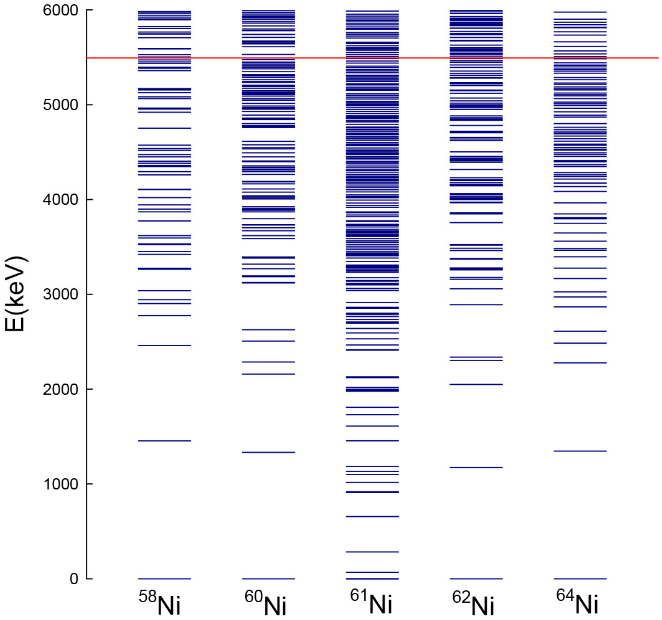

Figure 7. Known energy levels of the stable Ni isotopes (dark blue) in the vicinity of the HD/^{3}He transition near 5.5 MeV (red).

10.2. Impurity Nuclei

This draws attention to the start up problem within the model. When excess heat is being produced, then there is the possibility of making up energy mismatches at the keV or 10s of keV scale via up-conversion and down-conversion, in which case if some of the nearby levels of the nickel isotopes are reasonably stable then they can be candidates to participate in the overall reaction. However, before excess heat is being made, the question can be asked as how the process starts, since substantial up-conversion and down-conversion under these conditions seems unlikely. What is needed are long-lived states more nearly resonant, presumably from impurities in the nickel.

We can make use of the NUDAT2 database to ask what energy levels of the stable nuclei are known that are more closely resonant with the HD/^{3}He transition energy. Results from a search of this kind are shown graphically in Figure 8. Closest is the ^{116}Sn(5493.2) state, which looks like it may be within 300 eV (there are uncertainties involved since the known energies are reported to fewer digits than the HD/^{3}He transition is known). Note that there are many more nuclear energy levels in this region than what are tabulated in the database, as not all of the stable isotopes have been studied in this way in detail.

The conclusion is that within the overall proposed reaction scheme, excess heat in the NiH system would require some deuterium to be present, and would not be able to start up without impurity nuclei present in the Ni with nuclear states close to the HD/^{3}He transition energy. If correct, at some point in the future studies would be of interest in which specific impurity isotopes were present, from which it could be inferred have reasonably stable states near resonance at 5493.4780 keV.

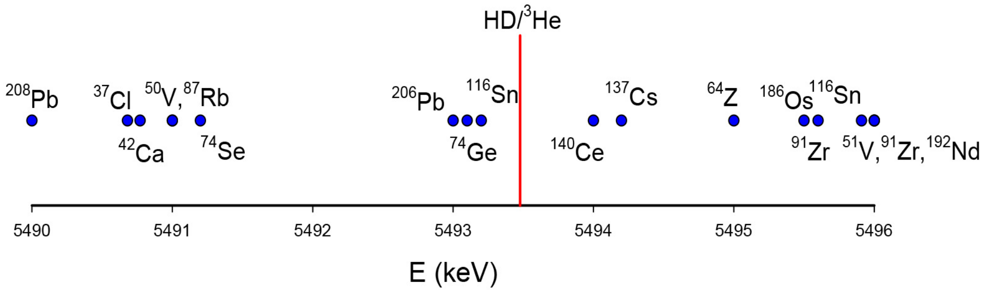

Figure 8. Known energy levels of stable isotopes (and ^{137}Cs) from the NUDAT2 database (blue circles) compared with the HD/^{3}He transition energy (red line).

11. ^{137}Cs and the HD/^{3}He Transition

The radioactive isotope ^{137}Cs beta decays to ^{137}Ba with the emission of an electron and an antineutrino with a half-life of 30.08 years. Most of the time this decay populates the excited state of ^{137}Ba at 661.659 keV (94.5%), and the rest of the time ground state ^{137}Ba is produced. The ^{137}Ba excited state decays produce a 661.657 keV gamma, which makes ^{137}Cs important as a calibration source for gamma spectroscopy.

11.1. Multiple Excitation Transfers

In the discussion above we found that ^{137}Cs has an excited state at 5494.2 keV, which is nearly resonant with the HD/^{3}He transition at 5493.4780 keV. The energy mismatch is less than 1 keV. Due to the phonon-nuclear interaction, indirect coupling would be expected between HD + ^{137}Cs(0), and ^{3}He+^{137}Cs(5494). We know almost nothing about this excited state in ^{137}Cs other than its energy. Most likely the coupling with this state would lead to gamma decay to some of the ^{137}Cs levels.

We might speculate that further excitation transfer can induce a coupling with longer-lived states of higher spin, for which beta decay is dominant (illustrated in Figure 9). In this case there is the possibility of seeing an overall acceleration of the beta decay of ^{137}Cs. Depending on the details of which states are produced from the beta decay of this highly-excited state, it is possible that an increase in the intensity of the 661.657 keV gamma might occur, as well as emission at other energies.

11.2. Possible Connection With Kornilova and Vysotskii Experiment

Kornilova, Vysotskii and coworkers have claimed a factor of 40 increase in the decay rate for ^{137}Cs in biological cultures measured from the time dependence of the 661 keV gamma [50]. It seems natural to consider whether the mechanism discussed in this section might be relevant.

Years ago we noted that under conditions where anomalous energy exchange is possible, that beta decay had the potential to be accelerated assuming that phonon exchange occurs. However, it seems unlikely that anomalous energy exchange would be possible in a biological culture, which would seem to rule out such a mechanism. In this case the near-resonance noted here may be a better candidate.

From the discussion above, it seems likely that if the near resonance is important then there may be additional gamma lines produced from highly-excited ^{137}Cs states that gamma decay rapidly. To account for a substantial acceleration in the beta decay rate, then excitation transfer to highly-excited ^{137}Cs states which beta decay faster than gamma decay likely occurs. There is the question as to what states are produced from the beta decay from these

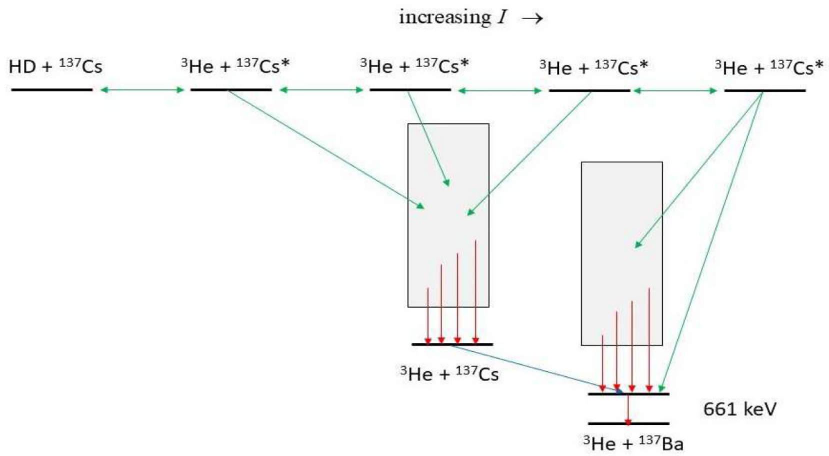

Figure 9. Schematic of how the HD/^{3}He transition might increase the decay rate for ^{137}Cs. The first excitation transfer step results in HD transitioning to ^{3}He and ground state ^{137}Cs transitioning to a nearby excited state, which would likely gamma decay to lower energy levels in ^{137}Cs (the grey box on the left). Repeated excitation transfer steps can lead to highly-excited states with higher total orbital and spin angular momentum, eventually leading to states where beta decay dominates over gamma decay, resulting in gamma decays to highly-excited states in ^{137}Ba (the grey box on the right) and possibly to the 661 keV state.

highly-excited ^{137}Cs. One might expect this beta decay to result in highly-excited states in ^{137}Ba, which would give rise to other gammas. What the yield is for the 661 keV gamma is an interesting question – one could imagine working with an initial known amount of ^{137}Cs and measuring the 661 keV emission before it is added to the biological culture, and then measuring again after it has been taken up into the cells. If a change in the 661 keV emission occurs, then this might be due to a finite yield of 661 keV emission resulting from the beta decay from highly-excited ^{137}Cs. If the mechanism under discussion is relevant, one might expect the decay rate to increase with a small addition of D_2O into the solution.

11.3. Possible Connection With the Piantelli Experiment

Piantelli and coworkers have described seeing gamma emission at 661.5 ± 0.8 keV in connection with their NiH excess heat experiments [51], [52]. There are issues in connection with these observations: whether the emission correlates with excess heat production or not; and whether the line is due to the well known transition in ^{137}Ba produced from ^{137}Cs or not.

In Table 2 we consider all known gamma transitions in the stable isotopes up to ^{137}Ba in the range 661-662 keV from the NUDAT2 database. There do not seem to be compelling candidates in general among this list, and no compelling candidates were proposed by the Piantelli group.

In connection with whether the line correlates with excess heat or not, during a visit to the Piantelli lab in 2011 the group demonstrated excess heat for Mike McKubre and I, and showed that the 661 keV line turned on when the excess heat turned on.

We would expect that when excess heat is produced, energy exchange beyond the few phonon or plasmon level becomes possible, so that the energy mismatch between the HD/^{3}He transition and the ^{137}Cs level at 5494.2 keV (or other levels) can be made up (this is illustrated in Figure 10). This has the potential to produce a stronger version of

Table 2. Excited state energies and gamma energies for all known gamma transitions between 661 keV and 661 keV among the stable isotopes up to ^{137}Ba.

isotope	E_j	E_γ
^{48}Ti	5974	662
^{50}Cr	3825.7	661.6
^{76}Ge	3409.19	661.4
^{75}As	860.0	661.4
^{77}Se	911.5317	661.719
^{88}Sr	8094.8	661.3
^{98}Mo	2419.63	661.12
^{98}Ru	3852.3	661.6
^{99}Ru	3536.29	661.76
^{102}Pd	5094.11	661.3
^{114}Cd	2525.420	661.21
^{120}Te	1863.29	662.0
^{126}Xe	3252.1	661
^{128}Xe	2941.9	661.0
^{137}Ba	661.659	661.657

the effect. The conjecture is that a small amount of ^{137}Cs was initially present in the nickel bar used in the experiment, and that its decay was dramatically increased leading to a large increase in the intensity of the 661 keV line.

11.4. ^{137}Cs as an Indicator of Anomalous Energy Exchange

If it is true that the intensity of the 661 keV line is sensitive to excess heat being produced, then this might be important for several reasons. It has the potential to provide for a very different kind of test for phonon-mediated and plasmon-mediated nuclear excitation transfer. It has the potential to provide information as to how much anomalous energy exchange occurs in connection with excitation transfer, under conditions where up-conversion and down-conversion occurs. The effect also has the potential to provide an independent diagnostic for heat production in light water excess

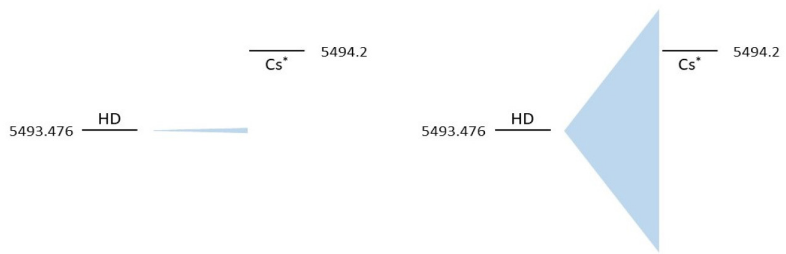

Figure 10. Simplified schematic of the the energy mismatch and lack of resonance in the absence of anomalous energy exchange (left); and the possibility of making up the energy mismatch between the HD/^{3}He transition and the nearby level in ^{137}Cs under conditions where anomalous energy exchange occurs (right), leading to a further acceleration of decay.

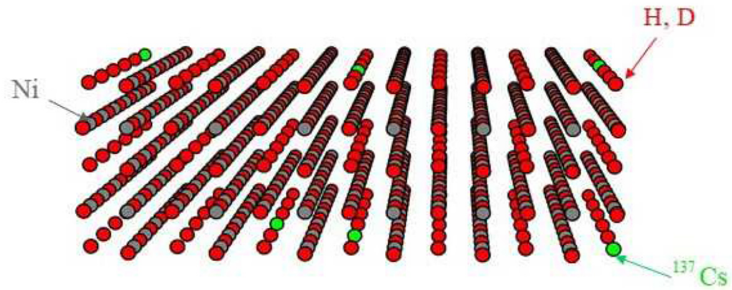

Figure 11. Illustration of ^{137}Cs going into vacancies in Ni co-deposited using the Letts protocol, assuming that locally we end up with a super-abundant vacancy phase.

heat experiments, which would be interesting and perhaps useful. There is the prospect for a mechanism that can be associated with the acceleration of radioactive decay, supporting the effort of Kornilova, Vysotskii and coworkers to remediate harmful radioactive isotopes. Although this mechanism has been discussed specifically in the context of the HD/^{3}He transition and ^{137}Cs, it is likely to work for other unstable isotopes as well.

How might this be tested? There are many possibilities. One approach might be to work with the Letts co-deposition with either Ni or Pd [53], which according to our earlier conjectures may make host metal atom vacancies [54]. If so, then the task would be to find a way to get ^{137}Cs into some of these vacancies (as illustrated in Figure 11). One possibility might be to arrange for ^{137}Cs to be in the electrolyte during the Ni or Pd co-deposition, hoping for a some of it to deposit. Another possibility might be to use different steps, where the Ni or Pd co-deposition is first done (in acid) following the Letts protocol. Then the surface could be rinsed off and placed in base, with electrolysis involving ^{137}Cs in the electrolyte. According to [55] Cs is found to go into the cathode at low levels during electrolysis in base. Then the surface could be rinsed, and then placed into a new cell for live tests. For this perhaps a small amount of Ni or Pd could be co-deposited, hoping to produce excess heat along with an increase in the 661 keV gamma line.

12. The Null Reaction

One of the first proposals for phonon-mediated excitation transfer years ago was for the null reaction [56], [57], in which a D_2 making a transition to ^{4}He at one site produced a new D_2 from a ^{4}He at another site (as illustrated in Figure 12). This process seemed of interest since it could be resonant, so that it could proceed as a coherent process. At the time this seemed to be of academic interest only, since it would seem to be hard to distinguish experimentally whether a D_2 at one site and ^{4}He at another site had undergone excitation transfer.

Our attention has recently returned to this problem motivated by the interpretation of the enhanced fusion rate observed in low-energy deuteron beam experiments, where the yield as a function of energy is fitted successfully to a model that includes a resonance at low energy [58]. The probability that a long-lived excited state of the alpha particle is nearly resonant at the eV level with D_2 seems low. On the other hand, excitation transfer from the D_2/^{4}He transition to produce p+t or n+^{3}He final state from ^{4}He seems like it might be a candidate explanation to account for the excess fusion rate observed at low beam energy.

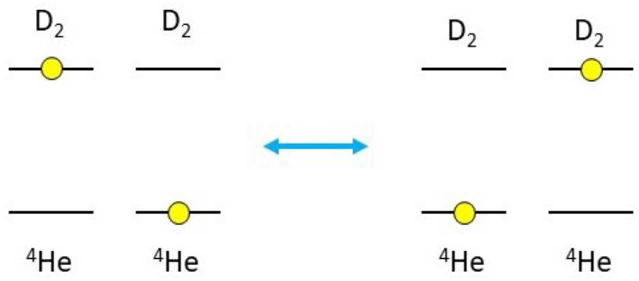

Figure 12. Concept of phonon-mediated nuclear excitation transfer in the case of the null reaction.

12.1. Simple Model

Let us consider a naive model for excitation transfer in the null reaction, where we might use a Hamiltonian of the form

$$\hat{H} = \hbar\omega_0 \hat{a}^\dagger \hat{a} + \sum_j \sum_k \frac{|\hat{\boldsymbol{\pi}}_{k|j}|^2}{m} + \sum_j \sum_{k<k'} V_{k,k'|j}$$

$$+\frac{1}{\Delta E_-}\sum_{j<j'}\Big|\mathrm{D}_2(j),\ {}^4\mathrm{He}(j')\Big\rangle\langle \mathrm{D}_2(j)|\hat{\mathbf{a}}_j\cdot c\hat{\mathbf{P}}_j|{}^4\mathrm{He}(j)\rangle\langle {}^4\mathrm{He}(j')|\hat{\mathbf{a}}_{j'}\cdot c\hat{\mathbf{P}}_{j'}|\mathrm{D}_2(j')\rangle\Big\langle\ {}^4\mathrm{He}(j),\ \mathrm{D}_2(j')\Big|$$

$$+\frac{1}{\Delta E_+}\sum_{j<j'}\Big|\ {}^4\mathrm{He}(j),\mathrm{D}_2(j')\Big\rangle\langle {}^4\mathrm{He}(j)|\hat{\mathbf{a}}_j\cdot c\hat{\mathbf{P}}_j|\mathrm{D}_2(j)\rangle\langle \mathrm{D}_2(j')|\hat{\mathbf{a}}_{j'}\cdot c\hat{\mathbf{P}}_{j'}|{}^4\mathrm{He}(j')\rangle\Big\langle \mathrm{D}_2(j),{}^4\,\mathrm{He}(j')\Big| \quad (27)$$

where we assume one highly-excited phonon mode, the relative nucleon kinetic energies (where k refers to a nucleon and j refers to a nucleus), the nucleon-nucleon interactions, and excitation transfer terms involving single-phonon exchange for all nuclear transitions.

There are technical issues associated with solving for the states of the system in this kind of model; however, after some thought it becomes clear that if a ^{4}He nucleus makes a transition to the D_2 channel it will initially be localized and not able to tunnel through the Coulomb barrier in a reasonable time. An approximation (not satisfying $P \to 0$ for $r \to 0$) for the resulting compact state spatial distribution is illustrated compared with the molecular D_2 state. The compact D_2 state is localized at the few fm scale. More work remains to develop a self-consistent compact state solution.

12.2. Compact D_2 State and the Kasagi Experiment

It might be asked whether such a compact D_2 state might be connected with experiment. An immediate application is to the three-body fusion experiment of Kasagi and coworkers [59], in which an incoming deuteron leads to energetic alpha and proton particles with an energy distribution consistent with a three deuteron fusion process. A confirmation of this result was reported in [60]. The compact D_2' state on the fermi scale discussed above could be involved in a reaction of the form

$$\mathrm{d} + \mathrm{D}_2' \longrightarrow \alpha + \mathrm{p} + \mathrm{n} + 21.62\ \mathrm{MeV}$$

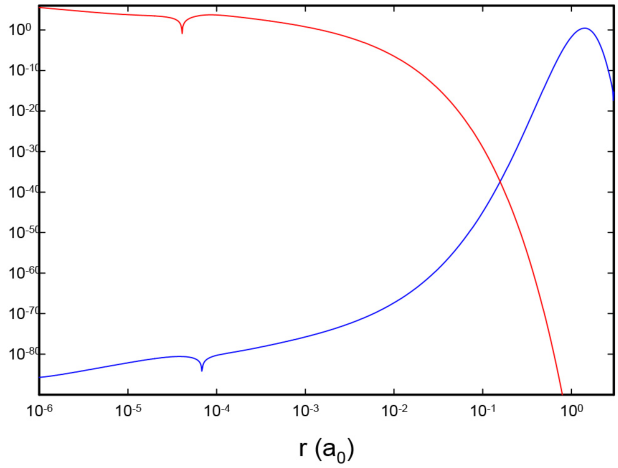

Figure 13. Approximate radial squared probability densities ($P^2(r)$) for an $l = 1$ D_2 state (blue, outer) and for an $l = 1$ compact state (red, inner).

A better notation for the same reaction in this case might be

$$\text{d} + (\text{dd})_{compact} \longrightarrow \alpha + \text{p} + \text{n} + 21.62 \text{ MeV}.$$

12.3. Deuteron-Deuteron Fusion Products

Based on the discussion above, there appear to be multiple ways in which dd-fusion products could be produced. The route simplest in concept could be written as a two-site excitation transfer reaction

$$\text{D}_2 + {}^4\text{He} \begin{cases} \nearrow & {}^4\text{He} + n + {}^3\text{He} + 3.27 \text{ MeV} \\ \rightarrow & {}^4\text{He} + \text{D}_2' \\ \searrow & {}^4\text{He} + p + t + 4.03 \text{ MeV} \end{cases}$$

where the D_2' state is compact as discussed above. We might expect this process to be inefficient at producing low-level p+t and n+^{3}He fusion products since the final states associated with this kind of excitation transfer process are so unstable. The compact D_2' state is unstable against 24 MeV gamma decay (how unstable depends on the details of precisely which LSJ states are involved). The longer-lived the state, the more likely that excitation transfer will result in occupation of the state.

There is a related but more complicated route to the formation of dd-fusion products where the first step in the process is the formation of a compact D_2' species. We might write this as a three-site excitation transfer reaction

$$\mathrm{D}_2 +^4 \mathrm{He} +^4 \mathrm{He} \begin{matrix} \nearrow \\ \rightarrow \\ \searrow \end{matrix} {}^4\mathrm{He} + \mathrm{D}_2' +^4 \mathrm{He} \begin{matrix} \nearrow & {}^4\mathrm{He} +^4 \mathrm{He} + n +^3 \mathrm{He} + 3.27\ \mathrm{MeV} \\ \rightarrow & {}^4\mathrm{He} +^4 \mathrm{He} + \mathrm{D}_2' \\ \searrow & {}^4\mathrm{He} +^4 \mathrm{He} + p + t + 4.03\ \mathrm{MeV} \end{matrix}$$

The idea here is that the formation of dd-fusion products starting from a compact state D_2' may be more efficient, since the relevant phonon-nuclear matrix element for the $\mathrm{D}_2'/^4\mathrm{He}$ transition is much larger.

Testing whether these processes are responsible for the production of low-level dd-fusion products would seem to involve controlling how much $^4\mathrm{He}$ is in the sample, and then checking on the dependence of the reaction rate on $^4\mathrm{He}$ concentration.

12.4. First Step in the Excess Heat Process

In the Introduction we described a complicated coherent reaction scheme for excess heat production in the PdD system (Figure 1). A weakness of this proposed scheme is that the first excitation transfer step requires a relatively long-lived highly-excited state in the vicinity of 24 MeV, which on the face of it seems to be unlikely. In light of the discussion in this section it seems clear that this first step could be replaced with an excitation transfer that results in a compact D_2' state instead, which is expected to be much more stable. A modification of the coherent reaction scheme to include this is shown in Figure 14.

12.5. Low-Level Energetic Particle Emission

The phonon-nuclear coupling matrix element is orders of magnitude stronger for the compact state $\mathrm{D}_2'/^4\mathrm{He}$ transition than for the molecular $\mathrm{D}_2/^4\mathrm{He}$ transition, which would be expected to impact the transfer to highly-excited states of

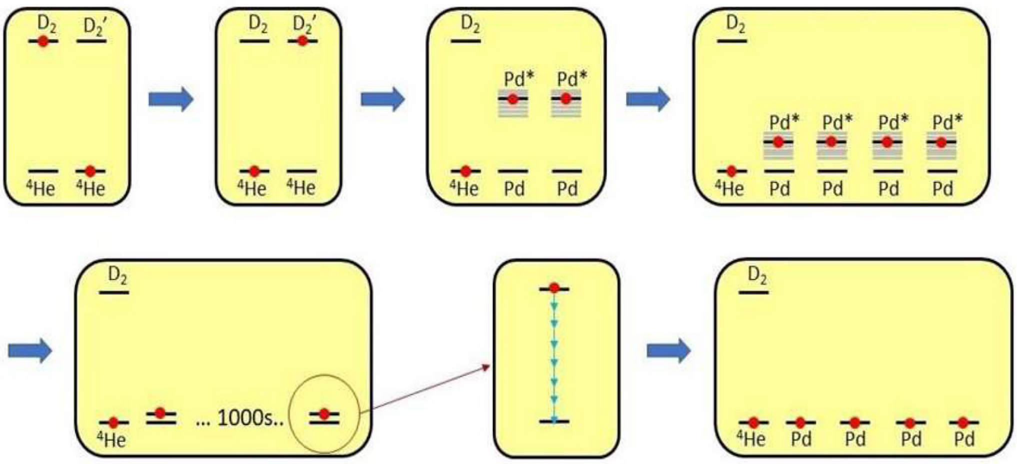

Figure 14. Schematic of the revised version of the model for excess heat production where the first excitation transfer step results in a compact D_2 state (indicated as D_2' here).

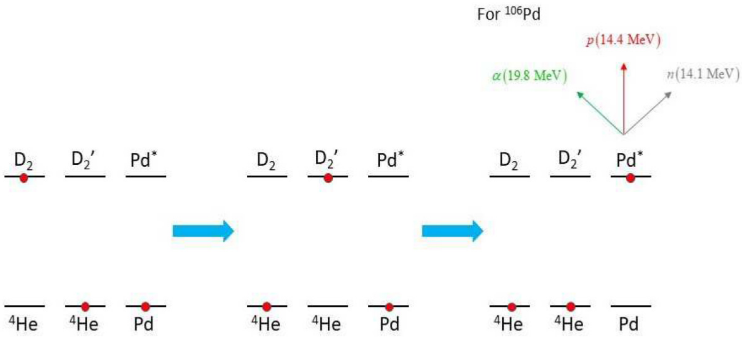

Figure 15. Schematic of excitation transfer of 24 MeV from the $D_2/^4He$ transition to a compact $D_2'/^4He$ transition resulting in a highly-excited state in ^{106}Pd that subsequently decays.

nuclei in the host lattice. The issue is that excitation transfer involving a small coupling matrix element to an unstable highly-excited state that decay rapidly is hindered; while excitation transfer from the compact $D_2'/^4He$ transition would involve a much larger coupling matrix element, and hence lead to a much larger probability of transfer and decay. As an example, we consider the associated modification of Figure 3 to include excitation transfer to produce a compact D_2' intermediate state prior to the excitation of a Pd nucleus in Figure 15.

13. Subdivision

Subdivision as we consider it involves multiple excitation transfer events that start with a single excited nucleus and result in two or more excited nuclei where the total excitation energy is (approximately) conserved [10], [11].

From the discussions above we see that subdivision is a key element in the overall reaction schemes proposed for excess heat in the Fleischmann-Pons experiment. In this section we are interested three issues: is there evidence in experiments done so far that subdivision occurs; can states be avoided in the first subdivision step in the proposed excess heat process; and is there a possibility that subdivision could be demonstrated in the lab, so that we could be certain that it occurs and so that we might be able to study it in simpler controlled laboratory experiments.

13.1. Subdivision and the $D_2/^4He$ Transition

The simplest reaction scheme for subdivision starting from the $D_2/^4He$ transition is

$$D_2 + {}^{A_1}Z_1 + {}^{A_2}Z_2 \quad \longleftrightarrow \quad {}^4He + {}^{A_1}Z_1^* + {}^{A_2}Z_2^*$$

where the 24 MeV transition energy is split to produce excitation in two lattice nuclei. Ideally the initial and final state energies are resonant, or can be made up by the exchange of a few phonons or plasmons. We would expect the highly-excited states produced to be unstable, which may help in arranging for the overall multi-step excitation transfer process to be on resonance.

In light of the discussion in the previous section, it may be that a compact D_2' state is formed as an intermediate state according to

$$D_2 + {}^4\text{He} + {}^{A_1}Z_1 + {}^{A_2}Z_2 \quad \longleftrightarrow \quad {}^4\text{He} + D_2' + {}^{A_1}Z_1 + {}^{A_2}Z_2 \quad \longleftrightarrow$$
$${}^4\text{He} + {}^4\text{He} + {}^{A_1}Z_1^* + {}^{A_2}Z_2^*$$

In both schemes the two excited nuclei that result subsequently decay incoherently. Extensions are also possible where subdivision occurs following more excitation transfers of the compact D_2' state among ^{4}He nuclei.

13.2. Simple Empirical Model for Subdivision

The evaluation of subdivision rates and products would require computational models for the highly-excited states/resonances including energies and lifetimes, as well as phonon-nuclear coupling matrix elements. We would expect that the overall subdivision rate will be larger if the two highly-excited final states are nearly energy resonant with the initial state, and if the decay rates are slow.

An accurate first principles calculation of the associated rates and distribution of products is hindered by limitations in our ability to carry out accurate structure, energy, and decay rates for the large number of highly-excited nuclear states in the continuum. Under such conditions is seem dubious that we should be able to make relevant predictions at all.

We defer these difficult accurate subdivision calculations, and consider here a much simpler approach. If it happens that a reasonably long-lived highly-excited state occurs with exactly half of the transferred energy, then a Dicke-enhanced subdivision would be possible. To expect that such a coincidence might be a common occurrence would not be reasonable; however, with such an ansatz it is possible to develop a very simple model with which we are able to begin a theoretical discussion. For example, if there are energetic particles close to what is predicted from such a model, then perhaps further work might be worthwhile to following up to see if the isotopes implicated contribute the products.

A specific empirical model can be developed according to

$$C(E) \; = \; \sum_j f_j e^{-(E-E_j)^2/\Delta E^2} \tag{28}$$

where $C(E)$ is the associated simple model prediction, and where the (optimized) f_j coefficients keep track of the weight of the contribution to the spectrum from isotope j. The energies E_j can be determined simply from the ansatz, and ΔE is a free parameter (potentially connected with the detector resolution) to be optimized.

13.3. Possible Subdivision in the Pd Isotopes

We first consider the Pd isotopes, where "ideal" subdivision to produce matched excited final states would lead to the alpha, proton and neutron energies listed in Table 3.

Neutron emission above 2.45 MeV was reported by Takahashi and coworkers [61], with evidence for neutrons between 4 MeV and 5 MeV. We digitized the data of Figure 2 in [61] using the WebPlotDigitizer of Ankit Rohatgi, and fit to the simple model. Results from the optimization, augmented with a contribution at 2.45 for the dd-fusion neutrons, is shown in Figure 16. The model in this case suggests that the neutrons in the 4-5 MeV band may be a result of subdivision in ^{105}Pd, and that some of the lower energy neutrons may be due to subdivision in other Pd isotopes.

An obvious experiment suggested by this model is to try looking for neutron emission in the 4-5 MeV region of the spectrum using a Pd sample made entirely of mass 105, and alternatively with a Pd sample in which no mass

Table 3. Alpha energies E_α, proton energies E_p and neutron energies E_n (including recoil) expected from decay of the Pd excited state formed under idealized subdivision where the final excited state energy is exactly half of the transferred energy.

isotope	E_α (MeV)	E_p (MeV)	E_n (MeV)
^{102}Pd	9.41	4.07	1.34
^{104}Pd	8.97	3.24	1.92
^{105}Pd	8.69	3.14	4.78
^{106}Pd	8.37	2.55	2.34
^{108}Pd	7.77	1.96	2.67
^{110}Pd	7.22	1.29	3.10

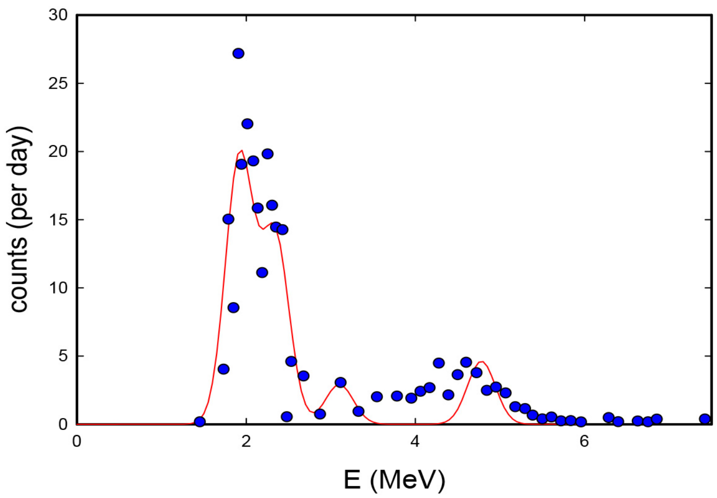

Figure 16. Plot of neutron data reported by Takahashi et al compared with the simple model described in the text for neutron emission from subdivision.

105 isotopes are present. If energetic neutrons in this part of the spectrum were correlated with ^{105}Pd this would be supportive of the proposed interpretation that subdivision is responsible for them.

13.4. Possible Subdivision in the Er Isotopes

A similar approach might be taken in the case of subdivision in the Er isotopes. In this case Er has six stable isotopes with alpha, proton and neutron decay energies given in Table 4 for ideal subdivision into identical excited states.

In this case we consider neutron emission for a deuterated Eu sample irradiated by gammas in the range 2.5-2.9 MeV [62], where the protons resulting from deuteron disintegration would be expected to produce THz vibrations capable of stimulating nuclear excitation transfer. We have digitized the data in Figure 5(a), and fitted it using

Table 4. Alpha energies E_α, proton energies E_p and neutron energies E_n (including recoil) expected from decay of the Er excited state formed under idealized subdivision where the final excited state energy is exactly half of the transferred energy.

isotope	E_α (MeV)	E_p (MeV)	E_n (MeV)
^{162}Er	13.24	5.46	2.72
^{164}Er	12.91	5.04	3.06
^{166}Er	12.45	4.58	3.43
^{167}Er	12.29	4.39	5.45
^{168}Er	12.18	3.90	4.13
^{170}Er	11.69	3.30	4.64

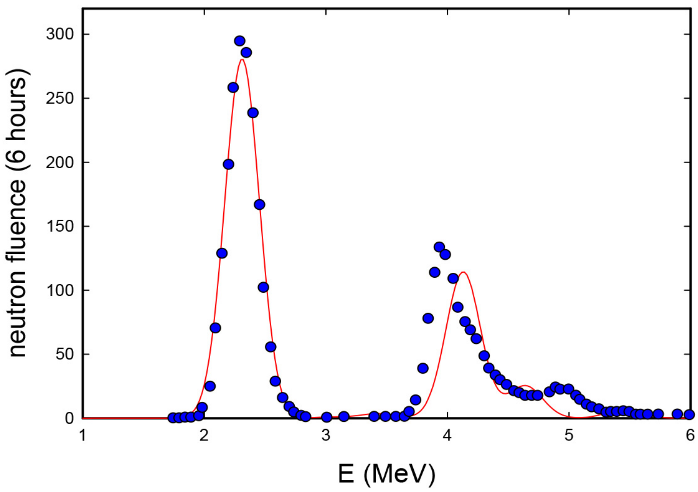

Figure 17. Plot of neutron data reported by Steinetz et al compared with the simple model described in the text for neutron emission from subdivision. For this model we allowed the dd-fusion energy to be determined from the data rather than fixing it at 2.45 MeV.

the empirical subdivision model, augmented by a contribution for 2.45 MeV dd-fusion neutrons (allowing the center energy to be determined from the data). Results are shown in Figure 17.

A conclusion from this is that there are subdivision candidates in the vicinity of the observed neutron peaks at higher energy, and that symmetric subdivision in ^{168}Er is a candidate to account for the peak near 4 MeV. As above, to provide clarification of this point we would like to have similar experimental results involving a sample composed of ^{168}Er, and a sample with no ^{168}Er.

13.5. Avoiding Very Unstable Excited States

Note that there may also be a potential problem finding reasonably stable states after one subdivision resulting in two excited states each with roughly half the transferred 24 MeV energy quantum. The speculation here is that if the first subdivsion from the compact D_2' state results in four excited states with lower excitation, then the resulting excited states may be much more stable. A schematic of how this might work in the case of the initial subdivision resulting in four excited states is shown in Figure 18.

13.6. Subdivision at Lower Energy

The discussion above has been concerned with subdivision in the case of the large 24 MeV quantum associated with the D_2/^{4}He transition; however, we note that in the various proposed schemes for coherent reactions for excess heat production that successive subdivisions are required for part of the down-conversion of the large quantum. This suggests that a study of subdivision at lower energy would be useful. Very convenient would be subdivision implemented in experiments similar to those which have been studied for excitation transfer [21]–[23].

We have considered possible subdivision reactions in which an initial nuclear excited state is produced following the decay of a (commercially available) radioactive isotope that decays to produce excited states in two other nuclei. If the process were resonant, then the initial excitation energy would match the sum of the two excitation energies of the final state nuclei. A computer code was developed to search low-lying (below 250 keV) excited states of the stable nuclei for resonances, and a modest number of candidates were identified [63]. We do not have confidence that the mismatch could be made sufficiently small in any of the candidate sets of transitions that the mismatch could be made up through the exchange of a few phonons. However, it does seem possible to arrange for subdivision where the energy mismatch is made up through the exchange of a few photons (the idea here is that optical photons couple to plasmons which mix with phonons).

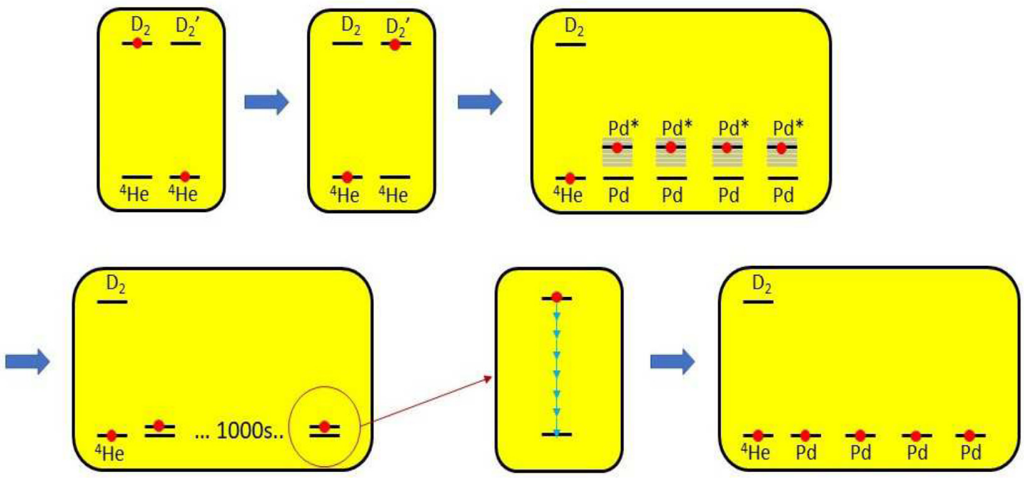

Figure 18. Schematic of a model for excess heat production where the first excitation transfer step results in a compact D_2' state and where the first subdivision step leads to four excitations.

Table 5. Candidate photon energies around which to scan under the assumption that different numbers of photons are absorbed. In the second row we do not list the $\Delta n = \pm 6$ case since that is higher order since two of the transitions are E1 (one-phonon) and one is an E2 (two-phonon) transition.

${}^AZ_i$	E_i (keV)	${}^AZ_{f1}$	E_{f1} (keV)	${}^AZ_{f2}$	E_{f2} (keV)	$\hbar\omega_0$ $\Delta n = \pm 2$	$\hbar\omega_0$ $\Delta n = \pm 4$	$\hbar\omega_0$ $\Delta n = \pm 6$
^{123}Te	159.024	^{158}Gd	79.5143	^{158}Gd	79.5143	2.30 eV	1.15 eV	0.77 eV
^{155}Gd	105.3106	^{181}Ta	6.237	^{183}W	99.0791	2.75 eV	1.37 eV	–
^{57}Fe	136.4743	^{155}Gd	60.0106	^{174}Yb	76.471	3.65 eV	1.82 eV	1.22 eV
^{85}Rb	151.192	^{159}Tb	57.9964	^{178}Hf	93.1803	7.65 eV	3.82 eV	2.55 eV

In Table 5 we list four candidate sets of transitions which are close to resonance, where the energy mismatch is balance by photon exchange according to

$$E_i \;=\; E_{f1} + E_{f2} + \Delta n \hbar\omega_0. \tag{29}$$

14. Phase Coherence With Resonant Excitation Transfer

We have been working on excitation transfer experiments in which ^{57}Co decays to produce excited states in ^{57}Fe, and then looking for changes in the gamma and x-ray emission following stimulation with (stress-induced) THz vibrations [21]–[23]. We were interested in developing a simulation model that could be used to model the experiment, and perhaps to begin a quantitative comparison of theory with experiment. Such a project is hindered from a basic lack of understanding of exactly where the THz vibrations are produced (a possibility is in the relative motion of the epoxy on top of the evaporated ^{57}Co/^{57}Fe deposit), what frequencies are involved, and how strong the vibrations are. What is really needed is a simpler experiment that is easier to model and to understand.

14.1. Phonon-Nuclear Interaction

We consider the first few steps in the development of a model for a different nucleus – one involving an electric dipole (E1) nuclear transition, so that only one phonon needs to be exchanged when a nuclear transition occurs (nuclear transitions in ^{57}Fe involve two-phonon exchange, so the model will be more complicated). The key to modeling this new system is the phonon-nuclear interaction. The relevant part of the Hamiltonian can be written as

$$\hat{H}_{int} \;=\; \sum_j \hat{\mathbf{a}}_j \cdot c\hat{\mathbf{P}}_j \tag{30}$$

The $\hat{\mathbf{a}}_j$ operator acts on the internal nuclear degrees of freedom of nucleus j, which for this discussion allows for a transition from one nuclear state to another. In the case of resonant excitation transfer, this operator mediates a transition between the excited state and the ground state. The $\hat{\mathbf{P}}_j$ operator creates or destroys one phonon when a nuclear state change occurs.

14.2. Resonant Excitation Transfer

Consider now a resonant excitation transfer process for an excited nucleus that has just been formed as a result of the beta decay of an appropriate radioactive source nucleus. The interaction above can cause the excited nuclear state to make a transition to the ground state, coupling to an off-resonant state where there are no excited nuclei. A subsequent interaction can bring the system back into resonance by raising another ground state nucleus to the excited state, where the phonon exchange in both cases has to be from the same phonon mode, one creation and one annihilation so that there is no net change in the phonon energy. If so, then the new excited nucleus will be formed within a few hundred Angstroms of where the original one started, since the coherence domain of a THz phonon is not very large.

If phonon-mediated nuclear excitation transfer worked conventionally, then the contributions from all of the different phonon modes would destructively interfere so that excitation transfer would be restricted to nearest neighbor nuclei. However, since nuclear states shift off of resonance, this destructive cancellation can in part be removed, leading to a much larger delocalization if there happens to be a highly-excited phonon mode.

14.3. Beam Formation in an Ordered Lattice

If the highly-excited phonon mode has a long wavelength (on the order of the size of the coherence domain), then the excited nuclei at the different locations will have the same phase. Assuming local order, then this phase coherence will lead to beam formation very similar to what happens in crystal diffraction experiments. In the ^{57}Fe experiments done in our experiments there was likely local order; however, the local crystal orientation likely varies over the different parts of the sample, so that it would not be expected for a macroscopic sample to produce a directed beam.

This suggests that a better way to do a resonant excitation transfer experiment is to work with a sample with macroscopic order, such as would occur with a single crystal sample (see Figure 19). For such a sample resonant excitation transfer in the case of a long wavelength phonon mode would produce beamlets as illustrated in Figure 20. If the vibrational mode wavelength is not long, then we might expect a modulation of the amplitude of the occupation probability for the excited nuclei, resulting in a modification of the angular emission pattern.

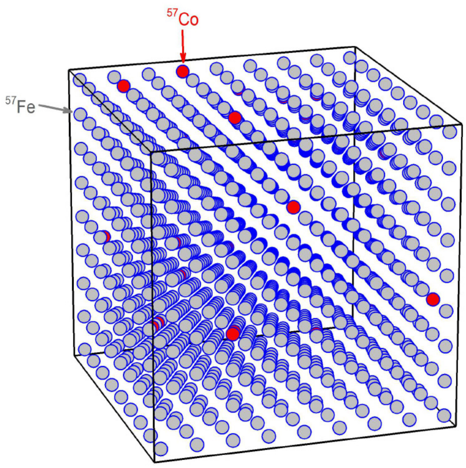

Figure 19. Proposal for a ^{57}Co/^{57}Fe resonant excitation transfer experiment making use of a single crystal sample.

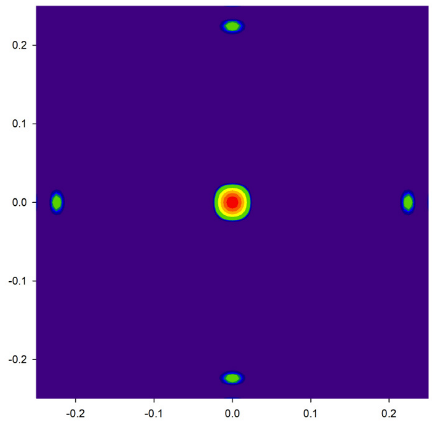

Figure 20. Beamlets produced around the [100] direction from the decay of 136 keV nuclei with phase coherence, with angles in radians.

15. Thoughts on a Model for Excess Heat Production

The discussion in the sections above provide a picture for how excess heat might be produced in the Fleischmann-Pons experiment. The question is whether this picture can be translated into a quantitative model that can be evaluated to give predictions for specific experiments.

15.1. Practical Issues

The number of issues involved is very large. As a practical matter, modeling sequential subdivision among the excited states of Pd nuclei (or impurity nuclei) will be hindered by a lack of precise state energies and wave functions with which to evaluate the phonon-nuclear matrix elements. Modeling down-conversion will be hindered in general by a lack of knowledge of precisely which low-energy nuclear transitions are involved, or in most cases which vibrational modes are involved.

Given this situation, what might be possible is to make use of lists of known nuclear levels with which to assemble a candidate set of subdivisions, and then develop estimates for the phonon-nuclear coupling matrix elements. Another approach might be to carry out moderately large nuclear structure calculations for the different isotopes, from which a set of (representative) phonon-nuclear matrix elements can be assembled.

For the down-conversion part of the model, it might be possible to work with an excess heat experiment in which an impurity is added which has a known low-energy transition, in which a down-conversion based on that transition may be relevant. This might be combined with a diagnostic (such as in Ref. [64]) to provide input about which phonon modes are involved.

15.2. One Approach to Putting Things Together

Assuming that an appropriate set of input data can be assembled for such a model, there remains more issues to be dealt with. A key motivation for pursuing this kind of model is the possibility that the dynamics will be coherent in the sense of Rabi oscillations. We need a formulation of the problem that works this way.

Conceptually simple might be an approach which starts with finite basis matrix equations of the form

$$E\mathbf{c} = \mathbf{H} \cdot \mathbf{c} \tag{31}$$

and decompose into

$$\begin{aligned} E\mathbf{c}_i &= \mathbf{H}_{ii} \cdot \mathbf{c}_i + \mathbf{H}_{ij} \cdot \mathbf{c}_j \\ E\mathbf{c}_j &= \mathbf{H}_{jj} \cdot \mathbf{c}_j + \mathbf{H}_{ji} \cdot \mathbf{c}_i + \mathbf{H}_{jf} \cdot \mathbf{c}_f \\ E\mathbf{c}_f &= \mathbf{H}_{ff} \cdot \mathbf{c}_f + \mathbf{H}_{fj} \cdot \mathbf{c}_j \end{aligned} \tag{32}$$

where $\mathbf{c}_i$ contains the initial state, where $\mathbf{c}_j$ includes intermediate states, and where $\mathbf{c}_f$ contains the final state. Then the intermediate states could be eliminated

$$\mathbf{c}_j = \left(E - \mathbf{H}_{jj}\right)^{-1} \cdot \left(\mathbf{H}_{ji} \cdot \mathbf{c}_i + \mathbf{H}_{jf} \cdot \mathbf{c}_f\right) \tag{33}$$

leading to

$$\begin{aligned} E\mathbf{c}_i &= \mathbf{H}_{ii} \cdot \mathbf{c}_i + \mathbf{H}_{ij} \cdot \left(E - \mathbf{H}_{jj}\right)^{-1} \cdot \left(\mathbf{H}_{ji} \cdot \mathbf{c}_i + \mathbf{H}_{jf} \cdot \mathbf{c}_f\right) \\ E\mathbf{c}_f &= \mathbf{H}_{ff} \cdot \mathbf{c}_f + \mathbf{H}_{fj} \cdot \left(E - \mathbf{H}_{jj}\right)^{-1} \cdot \left(\mathbf{H}_{ji} \cdot \mathbf{c}_i + \mathbf{H}_{jf} \cdot \mathbf{c}_f\right) \end{aligned} \tag{34}$$

In this kind of formulation an indirect coupling matrix between initial and final states could be defined according to

$$\mathbf{H}_{fi} = \mathbf{H}_{fj} \cdot \left(E - \mathbf{H}_{jj}\right)^{-1} \cdot \mathbf{H}_{ji} \tag{35}$$

The matrices involved in a realistic model would be expected to be large, but this might provide a way to think about the problem and to perhaps develop quantitative estimates.

15.3. Another Approach

The approach outlined above might be considered a standard and general approach in which intermediate states can be eliminated algebraically. We might expect there to be difficulties in the event that some of the intermediate states have the same energy as the initial and final state, as the matrix inverse would become nearly singular. In this case an alternate approach might be more appropriate. In this case we can decompose the vector $\mathbf{c}$ into a component $\mathbf{a}$ involving degenerate states and a component $\mathbf{b}$ involving nondegenerate states. For this separation we can write

$$\begin{aligned} E\mathbf{a} &= \mathbf{H}_{aa} \cdot \mathbf{a} + \mathbf{H}_{ab} \cdot \mathbf{b} \\ E\mathbf{b} &= \mathbf{H}_{bb} \cdot \mathbf{b} + \mathbf{H}_{ba} \cdot \mathbf{a} \end{aligned} \tag{36}$$

States off of resonance can be eliminated according to

$$\mathbf{b} \;=\; \left(E - \mathbf{H}_{bb}\right)^{-1} \cdot \mathbf{H}_{ba} \cdot \mathbf{a} \tag{37}$$

leading to

$$E\mathbf{a} \;=\; \mathbf{H}_{aa} \cdot \mathbf{a} + \mathbf{H}_{ab} \cdot \left(E - \mathbf{H}_{bb}\right)^{-1} \cdot \mathbf{H}_{ba} \cdot \mathbf{a} \tag{38}$$

If the shift of basis states off of resonance is important, it can be included in this formulation according to

$$E\mathbf{a} \;=\; \mathbf{H}_{aa} \cdot \mathbf{a} + \mathbf{H}_{ab} \cdot \left(E - \mathbf{H}_{bb}(E)\right)^{-1} \cdot \mathbf{H}_{ba} \cdot \mathbf{a} \tag{39}$$

For this kind of model there is no direct coupling matrix between initial and final states. Instead it would be possible to develop a dynamic model for the evolution of the nearly degenerate states starting with occupation of the initial state.

15.4. Loss

In the models outlined briefly above the basic description is Hamilonian based and loss-free. We would expect loss mechanisms to be important, including decay channels for the nuclear states and phonon loss from highly-excited THz phonon modes which drive the nuclear dynamics.

There are two approach that may be useful. In one approach we might work with a non-Hermitian model where loss is included by augmenting the real Hamiltonian matrices above with complex parts that model the loss. In this case the basic formulation remains the same, except that the linear algebra will be complex.

The other approach retains an underlying loss-free Hermitian model, but then adds loss to density matrix equations derived from the Hamiltonian for the degenerate states. The challenge in this case is that we expect the Hamiltonian models to be large, which means that the associated density matrix version of the model will be much larger.

16. Discussion and Conclusions

Excess heat in Fleischmann-Pons experiments is a real physical effect worthy of scientific investigation. In this paper we have summarized our approach to the development of theoretical models that are relevant. For excess heat production the approach which is most promising is illustrated in Figure 18. This scheme is pretty complicated, involving nuclear excitation transfer, nuclear subdivision, and the down-conversion of nuclear excitation into a great many phonons.

Understanding whether this approach is correct or not must involve understanding of the different parts of the model and comparing theory with experiment. In our view a foundation of the model is a novel relativistic phonon-nuclear interaction, one which has not at this point been of interest in the mainstream literature, and which needs experimental confirmation. Of interest is the development of new excitation transfer experiments that are more easily compared with theory, and corresponding quantitative theoretical models which can be tested in detail against experiment. From such tests it should be possible to tell whether this phonon-nuclear interaction is dominant, and whether we can rely on it for the development of predictive models.

We would like to develop quantitative predictions for models for excitation transfer, subdivision, down-conversion, and for excess heat, and then apply these models to experiment. As is clear from the discussions above this will involve considerable work. And as is also clear, some progress has been made in recent years.

16.1. On a comment from a reviewer

A reviewer made the comment: "It seems to me that the article would become more convincing if the author showed on the basis of an analysis of specific successful experiments, where exactly his theory is better for justifying these experiments than alternative theories." There is no question that quantitative analyses of many experiments based on the models under development is desirable, and would be compelling if agreement were obtained. The bottom line is that in spite of decades of development, more work remains to be done (both theoretically and experimentally) before we get there. One issue is that we still need nuclear matrix element and off-resonant energy shift calculations (or empirical estimates). We are also going to need models for the phonon distributions in the THz regime produced in electrochemical experiments, discharge experiments and gas loading experiments. And we are going to need simulation codes that implement the models and include the necessary physics to model important features of experiments.

References

[1] M. Fleischmann, S. Pons and M. Hawkins, "Electrochemically induced nuclear fusion of deuterium," *Journal of Electroanalytical Chemistry and Interfacial Electrochemistry* **201** (1989) 301–307; errata **263** (1990) 187.

[2] M. Fleischmann, S. Pons, M. W. Anderson, L. J. Li and M. Hawkins, "Calorimetry of the palladium-deuterium-heavy water system," *Journal of Electroanalytical Chemistry and Interfacial Electrochemistry* **287** (1990) 293-348.

[3] J. R. Huizenga, *Cold Fusion. Fiasco of the century*, Oxford University Press (1994)

[4] A. Kitamura, A., A. Takahashi, K. Takahashi, R. Seto, T. Hatano, Y. Iwamura, T. Itoh, J. Kasagi, M. Nakamura, M. Uchimura, H.Takahashi, S. Sumitomo, T. Hioki, T. Motohiro, Y. Furuyama, M. Kishida, H. Matsune, "Excess heat evolution from nanocomposite samples under exposure to hydrogen isotope gases. Int," *J. Hydrogen Energy* **43** (2018) 16187–16200.

[5] A. Takahashi1, T. Yokose, Y. Mori, A. Taniike, Y. Furuyama, H. Ido, A. Hattori, R. Seto and J. Hachisuka, "Enhancement of excess thermal power in interaction of nano-metal and H(D)-gas,"*Proceedings of JCF20* (2019) 9–27.

[6] A. Takahashi, H. Ido, A. Hattori, R. Seto, A. Kamei, J. Hachisuka, T. Yokose, Y. Mori, A. Taniike and Y. Furuyama, "Latest progress in research on AHE and circumstantial nuclear evidence by interaction of nano-metal and H(D)-gas," *J. Condensed Matter Nucl. Sci.* **33** (2020) 14–32.

[7] F. Tanzella, R. George and R. Godes, "Nanosecond pulse stimulation in the Ni-H_2 system," *J. Condensed Matter Nucl. Sci.* **29** (2019) 202–210.

[8] F. Tanzella, R. Godes, J. Liu and R. George, "Mass and heat flow calorimetry in Brillouin's reactor," *J. Condensed Matter Nucl. Sci.* **33** (2020) 33–45.

[9] P. L. Hagelstein, "Bird's eye view of phonon models for excess heat in the Fleischmann-Pons experiment," *J. Condensed Matter Nucl. Sci.* **5** (2012) 169–180.

[10] P.L. Hagelstein, Models based on phonon–nuclear coupling, *Cold Fusion – Advances in Condensed Matter Nuclear Science*, J.P. Biberian (Ed.), Elsevier, Amsterdam (2020), pp. 283–297.

[11] P. L. Hagelstein, "Theory and experiments in Condensed Matter Nuclear Science," *J. Condensed Matter Nucl. Sci.* in press.

[12] S. E. Koonin and M. Nauenberg, "Calculated fusion rates in isotopic molecules," *Nature* **339** (1989) 690–691.

[13] M. L. E. Oliphant, P. Harteck and Lord Rutherford, "Transmutation effects observed with heavy hydrogen," *Proceedings of the Royal Society of London. Series A* **144** (1934) 692–703.

[14] P. L. Hagelstein and I. U. Chaudhary, "Energy exchange in the lossy spin-boson model," *J. Condensed Matter Nucl. Sci.* **5** (2011) 52–71.

[15] P. L. Hagelstein and I. U. Chaudhary, "Dynamics in the case of coupled degenerate states," *J. Condensed Matter Nucl. Sci.* **5** (2011) 72–86.

[16] P. L. Hagelstein and I. U. Chaudhary, "Second-order formulation and scaling in the lossy spin-boson model," *J. Condensed Matter Nucl. Sci.* **5** (2011) 87–101.

[17] P. L. Hagelstein and I. U. Chaudhary, "Local approximation for the lossy spin-boson model," *J. Condensed Matter Nucl. Sci.* **5** (2011) 102–115.

[18] P. L. Hagelstein and I. U. Chaudhary, "Coherent energy exchange in the strong coupling limit of the lossy spin-boson model," *J. Condensed Matter Nucl. Sci.* **5** (2011) 116–139.

[19] P. L. Hagelstein, "Quantum composites: A review, and new results for models for Condensed Matter Nuclear Science," *J. Condensed Matter Nucl. Sci.*, **20** (2016) 139–225.
[20] P.L. Hagelstein, Phonon-mediated nuclear excitation transfer, *J. Condensed Matter Nucl. Sci.* **27** (2018) 97–142.
[21] F. Metzler, P. L. Hagelstein and S. Lu, "Observation of non-exponential decay in x-ray and γ emission lines from Co-57," *J. Condensed Matter Nucl. Sci.* **27** (2018) 46–96.
[22] S. Lu, "Exploring Possible Coupling between Phonons and Internal Nuclear States," PhD Thesis (MIT) (2018).
[23] F. Metzler, *Experiments to Test for Phonon-Nuclear Interactions*, Master's Thesis (MIT) 2019.
[24] E. Wigner, "On unitary representations of the inhomogeneous Lorentz group," *Annals of Mathematics* **40** (1939) 149-204.
[25] V. Bargmann, "Irreducible unitary representations of the Lorentz group," *Annals of Mathematics* **48** (1947) 568-640.
[26] E. Wigner, "Invariance in physical theory," *Proceedings of the American Philosophical Society* **93** (1949) 521-526.
[27] P. A. M. Dirac, "Forms of relativistic dynamics," *Reviews of Modern Physics* **21** (1949) 392.
[28] E. P. Wigner, "Relativistic invariance in quantum mechanics," *Il Nuovo Cimento* **10** (1956) 517-532.
[29] L. L. Foldy, "Relativistic particle systems with interaction," *Physical Review* **122** (1961) 275.
[30] R. A. Krajcik and L. L. Foldy, "Relativistic center-of-mass variables for composite systems with arbitrary internal interactions," *Physical Review D* **10** (1974) 1777.
[31] P. L. Hagelstein, "Lowest order relativistic interaction between lattice vibrations and internal nuclear degrees of freedom," submitted to *Phys. Rev C*.
[32] P. L. Hagelstein, "Central and tensor contributions to the phonon-exchange matrix element for the $D_2/^4He$ transition," *J. Condensed Matter Nucl. Sci.* **11** (2013) 15–58.
[33] P. L. Hagelstein, "Calculation of the boosted spin-orbit contribution to the phonon-nuclear coupling matrix element of ^{181}Ta," *J. Condensed Matter Nucl. Sci.* **29** (2019) 392–400.
[34] S. Weinberg, "Effective chiral Lagrangians for nucleon-pion interactions and nuclear forces," *Nuclear Physics B* **363** (1991) 3–18.
[35] D. R. Entem and R. Machleidt, "Accurate nucleon-nucleon potential based upon chiral perturbation theory," *Physics Letters B* **524** (2002) 93–98.
[36] D. R. Entem and R. Machleidt, "Accurate charge-dependent nucleon-nucleon potential at fourth order of chiral perturbation theory," *Physical Review C* **68** (2003) 041001.
[37] R. Machleidt and D. R. Entem, "Chiral effective field theory and nuclear forces," *Physics Reports* **503** (2011) 1–75.
[38] P. L. Hagelstein, "Nonrelativistic reduction of the phonon-nuclear interaction for the one-pion exchange potential with pseudovector interaction," *J. Condensed Matter Nucl. Sci.* in press.
[39] P. L. Hagelstein, "Reduction of the $HD/^3He$ phonon-nuclear matrix element," *J. Condensed Matter Nucl. Sci.* in press.
[40] J. R. Stone and P. G. Reinhard, "The Skyrme interaction in finite nuclei and nuclear matter," *Progress in Particle and Nuclear Physics* **58** (2007) 587–657.
[41] E. Caurier, F. Nowacki, A. P. Zuker, G. Martinez-Pinedo, A. Poves and J. Retamosa, "Large scale diagonalization in the pf shell: Achievements and perspective," *Nuclear Physics* **A654** (1999) 747c–758c.
[42] G. P. Chambers, J. E. Eridon, K. S. Grabowski, B. D. Sartwell and D. B. Chrisey, "Charged particle spectra of palladium thin films during low energy deuterium ion implantation," *J Fusion Energy 9* (1990) 281–285.
[43] A. S. Roussetski, "Application of CR-39 plastic track detector for detection of DD and DT-reaction products in cold fusion experiments," *Proc. ICCF8* (2000) 253–257.
[44] G. P. Chambers, G. K. Hubler and K. S. Grabowski, "Search for energetic charged particle reaction products during deuterium charging of metal lattices," *AIP Conference Proceedings* **228** (1991) 383–396.
[45] G. P. Chambers, G. K. Hubler and K. S. Grabowski, "Evidence for MeV particle emission from Ti charged with low energy deuterium ions," *Naval Research Laboratory Report 6927* (1991).
[46] S A Lipinski and H U Lipinski, "Hydrogen-lithium fusion device, methods and applications," *United States Patent Application Publication* US 2009/0274256 A1 (2009).
[47] S A Lipinski and H U Lipinski, "Hydrogen-lithium fusion device," *WIPO/PCT Patent Application Publication* WO 2014/189799 A9 (2014).
[48] A. A. Sonzogni, "NuDat 2.0: Nuclear Structure and Decay Data on the Internet," *AIP Conference Proceedings* **769** American Institute of Physics (2005) 574–577.

[49] https://www.nndc.bnl.gov/nudat2/

[50] V. I. Vysotskii, A. B. Tashyrev, and A. A. Kornilova, "Experimental observation and modeling of Cs-137 isotope deactivation and stable isotopes transmutation in biological cells," *Low-Energy Nuclear Reactions Sourcebook*, American Chemical Society, Washington, DC. (2008) 295–309.

[51] S. Focardi, V. Gabbani, V. Montalbano, F. Piantelli and S. Veronesi, "Evidence of electromagnetic radiation from Ni-H systems," *Proc. ICCF11* (2004).

[52] S. Focardi and F. Piantelli, "Produzione di energia e reazioni nucleari in sistemi Ni-H a 400 C," *XIX Congresso Nazionale UIT* (2004).

[53] D. Letts and P. L. Hagelstein, "Modified Szpak protocol for excess heat," *J. Condensed Matter Nucl. Sci.* **6** (2012) 44–54.

[54] P. L. Hagelstein, "Molecular D_2 near vacancies in PdD and related problems," *J. Condensed Matter Nucl. Sci.* **13** (2014) 138–148.

[55] A. Czerwinski, M. Czauderna, G. Maruszczak, I. Kiersztyn, R. Marassi, S. Zamponi, "Influence of cesium cations on hydrogen and deuterium electrosorption in palladium," *Electrochimica acta* **42** (1997) 81–86.

[56] P. L. Hagelstein, "A unified model for anomalies in metal deuterides," *Proc. ICCF8* (2000) 363–374.

[57] P. L. Hagelstein, " A unified model for anomalies in metal deuterides," *Proc. ICCF9* (2002).

[58] K. Czerski, D. Weissbach, A. I. Kilic, G. Ruprecht, A. Huke, M. Kaczmarski, N. Targosz-Śleczka and K. Maass, "Screening and resonance enhancements of the ^{2}H(d, p)^{3}H reaction yield in metallic environments," *European Physics Letters* **113** (2016) 22001.

[59] J. Kasagi, T. Ohtsuki, K. Ishii and M. Hiraga, "Energetic protons and α particles emitted in 150 keV deuteron bombardment on deuterated Ti," *J. Phys. Soc. Japan* **64** (1995) 777–783.

[60] G. K. Hubler, K. S. Grabowski, D. L. Knies, R. A. Walker and P. L. Hagelstein, "Anomalous energetic proton emission during 170 keV deuteron bombardment of TiD_2," *J. Phys. Soc. Japan* **81** (2012) 124203.

[61] A. Takahashi, T. Takeuchi, T. Iida and M. Watanabe, "Emission of 2.45 MeV and higher energy neutrons from D_2O-Pd cell under biased-pulse electrolysis," *J. Nuclear Science and Technology* **27** (1990) 663–666.

[62] B. M. Steinetz, T. L. Benyo, A. Chait, R. C. Hendricks, L. P. Forsley, B. Baramsai, P. B. Ugorowski, M. D. Becks, V. Pines, M. Pines, R. E. Martin, N. Penney, G. C. Fralick and C. E. Sandifer II, "Novel nuclear reactions observed in bremsstrahlung-irradiated deuterated metals," *Phys. Rev. C* **101** (2020) 044610.

[63] P. L. Hagelstein, "Candidates for near-resonant subdivision experiments," *J. Condensed Matter Nucl. Sci.*, in press.

[64] M. R. Swartz, "Optical detection of phonon gain distinguishes an active cold fusion/LANR component," *J. Condensed Matter Nucl. Sci.* **20** (2016) 29–53.